Ad Hoc 802.11b Cooperative Protocols: Performance in a Slow Fading Channel

Niraj Agarwal, Divya ChanneGowda, Lakshmi Narasimhan Kannan, Marco Tacca, Andrea Fumagalli

Technical Report UTD/EE/02/2007
March 2007

Ad Hoc 802.11b Cooperative Protocols: Performance in a Slow Fading Channel

Niraj Agarwal, Divya ChanneGowda, Lakshmi Narasimhan Kannan, Marco Tacca, Andrea Fumagalli
The OpNeAR Laboratory
Erik Jonsson School of Engineering and Computer Science
The University of Texas at Dallas
E-mails: {nxa041000, dhc042000, lnk051000, mtacca, andreaf}@utdallas.edu

***Abstract*— This paper investigates the use of cooperative communications in the context of ad hoc IEEE 802.11b to combat radio signal degradations due to slow fading. The performance gain of both an existing cooperative protocol and the one proposed in the paper is discussed. It is quantitatively shown how much the two cooperative protocols increase throughput, lower delivery latency, and extend transmission span, when compared to the conventional IEEE 802.11b protocol. These features may help improve connectivity and network performance in ad hoc applications, where nodes' relative locations are difficult to control and predict.**

I. Introduction

WLAN's (wireless local area networks) have experienced tremendous growth and become the prevailing technology in providing wireless access to data users. The family of IEEE 802.11 protocols is perhaps the most widely accepted solution [1]. It must be noted that wireless links do not have well defined coverage areas, especially in ad hoc deployments. Propagation and channel characteristics are dynamic and unpredictable. Small changes in the node position or direction of mobility may result in significant differences in the signal strength. Adaptation to such conditions is a key issue in today's and future wireless communications.

One of the characteristics of the radio medium is its inherent broadcast nature. Besides the intended destination, a signal transmitted by a source may be received by other neighboring nodes that are within earshot. This broadcast nature of the radio medium can be used to improve the system throughput by having a node, other than the source and the destination, actively help deliver the data frame correctly. The cooperating node is referred to as the *relay*. The essence of the idea is that, the destination benefits from data frames arriving via two statistically independent paths, i.e., spatial diversity.

The advantages of cooperative communications include the ability to increase the radio channel capacity [2], [3], [4] and reduce the latency of automatic retransmission request protocols [5], [6], [7]. In [8] a IEEE 802.11b cooperative protocol is introduced to improve both throughput and latency of the medium access control (MAC). Data frames transmitted by the source are received by the relay, which in turn sends them to the destination. The destination acknowledges the received data frame directly to the source. The IEEE 802.11b cooperative protocol proposed in [8] is designed and studied to operate in fast fading channel, i.e., fading affects each received symbol independently of the other received symbols.

In this paper, cooperative communications in the context of IEEE 802.11b is further investigated assuming a slow fading channel, i.e., a flat Rayleigh channel, whereby the fading level is constant throughout the reception of the entire frame. The protocol is designed to operate in ad hoc mode only. Attempts to receive the data frame transmitted by the source are simultaneously made at both the relay and the destination. It is only when the destination is not successful in the reception attempt, that the relay sends the data frame again. The advantage of this approach is to limit the relay's intervention to those cases when the source transmission attempt is not successful in reaching the destination.

As discussed in the paper both cooperative MAC protocols (the one in [8] and the one proposed here) help cope with signal degradation due to slow fading. They provide higher throughput and lower latency when compared to the conventional IEEE 802.11b protocol. For a given throughput target, they achieve a maximum transmission span between the source and the destination that is up to 50% greater than one of the conventional IEEE 802.11b protocol. These features combined may help achieve improved connectivity and performance in ad hoc applications, where the nodes' relative locations are difficult to control and predict.

II. The Proposed Cooperative Protocol

This section describes the cooperative protocol proposed to enhance the performance of IEEE 802.11b. For simplicity, the protocol is described ignoring some control frames, e.g., the request to send (RTS), clear to send (CTS). The extension of the protocol description to include these additional control frames is straightforward.

Assume that three nodes have agreed to cooperate[1], i.e., source S, destination D, and relay R. The proposed cooperative MAC protocol is based on the distributed coordination function (DCF) defined for the ad hoc mode of the IEEE 802.11b standard. As shown in Fig. 1, when transmitting a data frame, S makes a direct attempt to reach D. While

This research is supported in part by NSF Grants No. ECS-0225528 and CNS-0435429.

[1]The protocol required to reach a consensus among the three nodes willing to cooperate is beyond the scope of this paper.

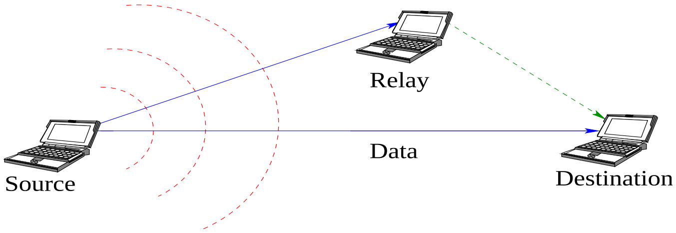

Fig. 1. Cooperation of three nodes : On Data frame

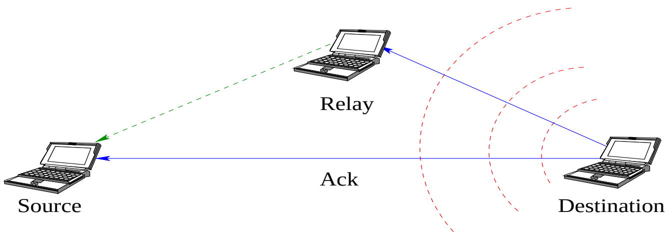

Fig. 2. Cooperation of three nodes : On ACK frame

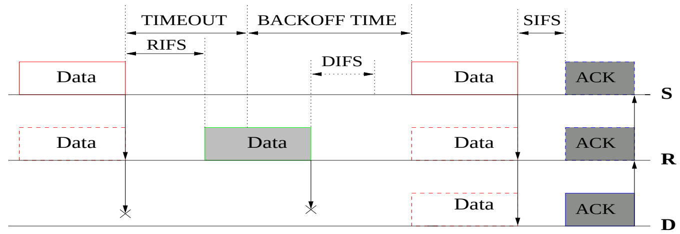

Fig. 5. Case 3: both S and R are unsuccessful

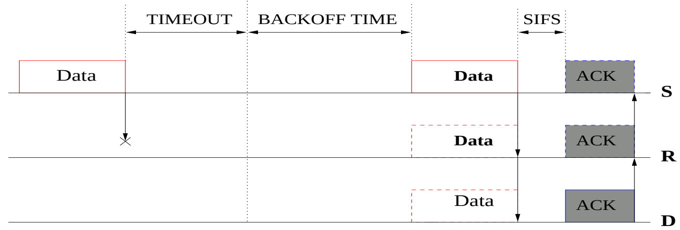

Fig. 6. Case 4: both D and R do not receive the data frame

transmission takes place, R receives and stores a copy of the data frame temporarily. Four cases are possible[2]. Their respective time diagrams of the transmitted frames are shown in Figs. 3-6.

1) Fig. 3: S transmitted frame is successfully received at D. D responds with a positive acknowledgment (ACK).
2) Fig. 4: S transmitted frame is successfully received at R, but not at D. D does not acknowledge the received data frame. R assumes that S's attempt to reach D has failed, and proceeds with the transmission of the data frame copy. R transmitted frame is successfully received at D. D responds to S with a positive ACK.
3) Fig. 5: Same as case 2, but D does not receive the frame transmitted by R.
4) Fig. 6: S transmitted frame is neither received successfully at R nor at D.

For the cooperation protocol to work as described, time intervals between transmission attempts must be chosen carefully. Specifically, for the transmission of a data frame, S must sense the channel idle and wait for a time interval denoted as distributed inter-frame space (DIFS)[3]. For ACK transmission, D needs not wait. ACK is then received at S and R no later than a time interval denoted as short inter-frame space (SIFS). SIFS takes into account various latency factors, e.g., MAC software, transceiver hardware, and radio signal propagation. Both DIFS and SIFS are defined in IEEE 802.11b. For transmission of the data frame copy, R must wait a time interval denoted as relay inter-frame space (RIFS). RIFS is specifically introduced as a component of the cooperative protocol and is not defined in IEEE 802.11b. RIFS must be chosen to both allow the detection at R of the ACK transmitted by D (RIFS $>$ SIFS), and prevent frame transmission of other nodes while the cooperation is taking place (RIFS $<$ DIFS). A possible value for RIFS is the point (coordination function) inter-frame space (PIFS). PIFS is defined in IEEE 802.11b to allow the point coordination function to have collision-free access to the channel for coordinating data frame transmissions in the infrastructure mode. Choosing RIFS=PIFS is a possible

[2]In the four cases it is assumed that the acknowledgment is always received correctly by S. The extension to account for acknowledgment loss is straightforward.

[3]Exception to this rule is when multiple frames containing the fragments of the same packet are sequentially transmitted by the same sender.

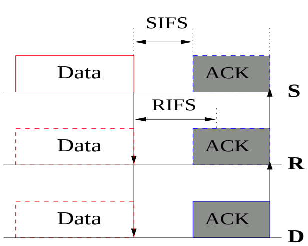

Fig. 3. Case 1: successful delivery of data and acknowledgement frames

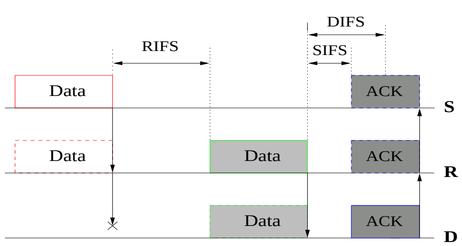

Fig. 4. Case 2: cooperation by R in retransmitting the data frame

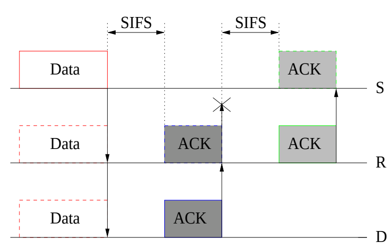

Fig. 7. Case 5: R helps in delivering the ACK frame

option when operating the cooperative protocol in the ad hoc mode, as the point coordination function is not present.

The backoff procedure at S is same as in IEEE 802.11b. When the predetermined maximum number of transmission attempts is reached, the data frame is discarded. Special attention is required to handle the transmission sequence of case 2 (Fig. 4). This is the case when the ACK is received long after a SIFS has elapsed since the data frame transmission ended at S. When ACK is not received after a SIFS, S starts the backoff procedure for either retransmission of the same data frame, or transmission of a new data frame if the maximum number of transmission attempts has been reached. However, the protocol is designed so that when R helps deliver the data frame to D, S receives ACK before it is able to make any new data frame transmission attempt. In this case, S stops the backoff procedure and resets the contention window.

During our study it was found that ACK reliability is an important issue and can significantly improve the throughput, especially if the nodes are far apart. This can be seen when the ACKs are made error free. The IEEE 802.11b and the UTD cooperative protocol were tested with error free ACKs. In the result section, the error free ACKs are tagged as $Bullet\ proofACKs$. It was found that $Bullet\ proofACKs$ gives significantly better throughput than the corresponding IEEE 802.11b and UTD cooperative protocol.

The ACKs can be made reliabe by sending the ACK at the lowest rate supported by IEEE 802.11b i.e. 1 Mbps. This ensures that ACKs are reliable if the nodes are within the range supported by 1 Mbps. However, when the distance between the nodes increases further, cooperation on the ACK frame can further increase the performance of the system. The UTD MAC II is deisgned considering the same. Cooperation on the ACK frame works as follows: When D wants to send ACK to the data frame sent by S, it attempts to send the ACK directly to S. R with high probability receives the ACK frame sent by D. After receiving the ACK, R waits for SIFS and sends the ACK again to S as shown in Fig.fig 2. S may get a duplicate ACK from R for the same data frame . This redundancy ensures that S receives the ACK if D's direct attempt to send the ACK to S fails. This is shown in Fig.fig 7 . If S and D are very close to each other, then with high probability S will receive the ACK from D. Thus R's attempt to send the duplicate ACK to S may become an overhead. Thus 2 way cooperation (UTD MAC-II) should be used if the channel between S and D is unfavorable. In the results section, UTD MAC-II is denoted as $2-way\ cooperation$ representing both cooperation on the data as well as the ACK frame.

As already mentioned, the proposed protocol does not change when RTS/CTS frames are considered. When R receives the RTS and/or CTS from S and/or D, it does not attempt transmission of its own data frames. However, it keeps listening and helps deliver the data frame from S to D whenever required.

The flowcharts of the cooperative protocol for S and R are shown in Figs. 8 and 9 respectively. As the flowcharts indicate, some changes are required in the MAC protocol for data transmission when compared to the IEEE 802.11b standard. No changes are required at D for data reception.

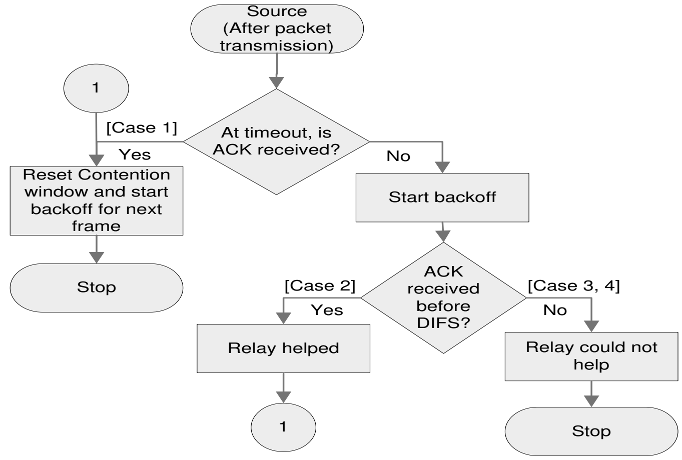

Fig. 8. Source's flowchart

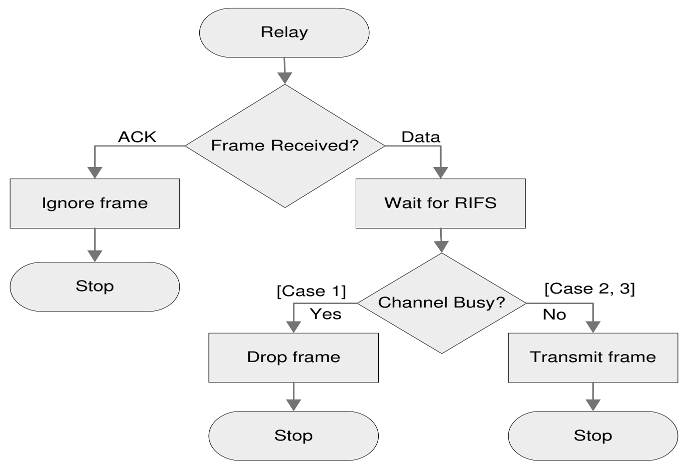

Fig. 9. Relay's flowchart

R must know the addresses of both S and D in order to relay data frames between the two nodes. Note that if traffic is bidirectional, R can help relay data frames in both directions. Conversely, S and D can function with or without R, and need not know R's address. Thus, the protocol and the data flow between S and D can smoothly adapt to changing channel conditions and relative locations of the three nodes.

The main difference between the protocol proposed in this section and the one in [8] is the attempt made by S to reach both D and R with the same frame transmission. The performance of both cooperative protocols is studied and compared against the conventional IEEE 802.11b protocol in the next section.

III. Results

In this section, simulation generated results are discussed to assess the performance gain in IEEE 802.11b when using cooperative protocols. In the study, three protocols are considered, i.e., the conventional IEEE 802.11b [9], MAC II in [8] (Poly MAC II), and the MAC protocol proposed in Section II (UTD MAC).

TABLE I
PARAMETERS USED IN SIMULATION

Path Loss Exponent	4
Flat Rayleigh Fading	constant across frame
Average Transmitter Power	100 mW
PHY Header	192 bits
SIFS	10 μs
RIFS	30 μs
DIFS	50 μs
Slot Time	20 μs
Vulnerable Period	20 μs
Max Retrans. Attempts	6
Frame Size	1023 bytes
Min Contention Window	31 slots
Max Contention Window	255 slots
Arrival Rate	1200 frames/s (saturation)
Arrival Distribution	Poisson
MAC Header	34 bytes
MAC ACK	14 bytes

The assumptions made and values chosen for the protocol parameters are shown in Table I. Three nodes are used, i.e., S, R, and D. Data flow is either from S to D only (one-way traffic), or bidirectional between S and D (two-way traffic). R does not generate any own traffic. It is assumed that the three nodes have agreed to cooperate. They can freely use any of the four transmission rates provided by IEEE 802.11b, i.e., 1, 2, 5.5, and 11 Mbps. However, ACK frames are always transmitted at 1 Mbps to provide maximum reliability.

The additive white Gaussian noise channel is used. Slow fading is modelled assuming that each frame is subject to a flat Rayleigh fading, independent of other frames. Fading is also independent of the destination, e.g., when S transmits, the fading experienced at R is independent of the one at D. Frame error rates are computed using [10]. Multiple concurrent transmission attempts always result in collision. Propagation delay is assumed negligible. The DCF mode of operation is used. Neither the virtual carrier sense (RTS/CTS) mechanism, nor fragmentation are used. The maximum number of transmission attempts per data frame is 6. Simulation results are obtained using a C++ custom simulator and have 5% confidence interval at 95% confidence level.

Saturation load condition is obtained by choosing data frame arrival rates that exceed the network capacity. Data frames in excess are dropped and not counted. Throughput is defined as the number of MAC payload bits that are successfully delivered and acknowledged by D normalized to time. The MAC and PHY header bits do not contribute to throughput. Access delay is the time taken for a data frame from the instant it reaches the head of the transmission queue at S till its first bit of the successful transmission attempt is aired by S. The Poly MAC II curves are obtained using the rules in [8], which establish when cooperation must be invoked and which transmission rates must be adopted by S and R respectively. The UTD MAC curves are obtained by selecting the transmission rates for S and R respectively, that jointly yield the maximal throughput for each experiment.

TABLE II
BIT RATE PAIRS FOR UTD MAC IN FIGS. 11 AND 12

S-R distance (m)	0-10	15-35	40-45	50-55	60	65-100
S Rate (Mbps)	1	11	11	5.5	5.5	2
R Rate (Mbps)	1	2	5.5	5.5	11	11

Cooperation in the UTD MAC is always invoked, regardless of the location of the three nodes.

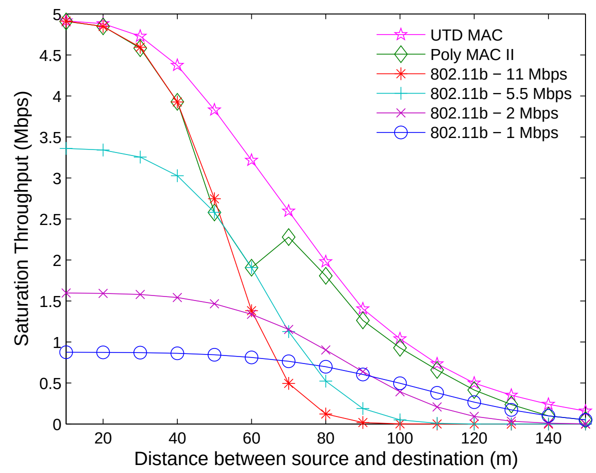

Fig. 10. Throughput vs. S-D distance, R is half way

Fig. 10 shows throughput under saturation load for the three protocols as a function of the distance between S and D. Traffic is one-way. Four curves are reported for IEEE 802.11b, one for each transmission rate. R is always placed half way between S and D to provide optimal condition for cooperation. Under this condition, the two cooperative protocols offer increased throughput when compared to IEEE 802.11b for distances of 40 m and above. Poly MAC II best contribution is reached at 70 m and above.

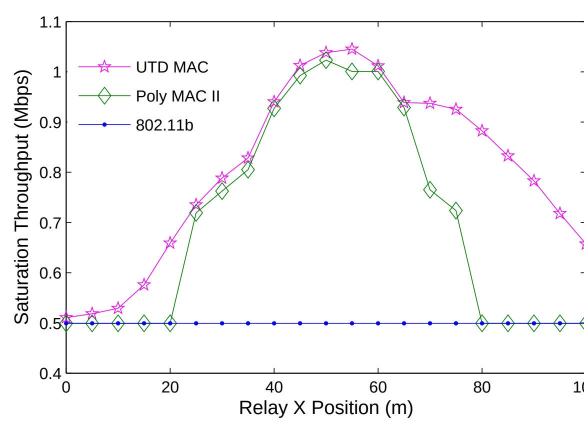

Fig. 11. Throughput vs. R's position along the S-D axis, S-D distance is 100 m

Figs. 11 and 12 show throughput and expected access delay respectively, under saturation load when the S-D distance

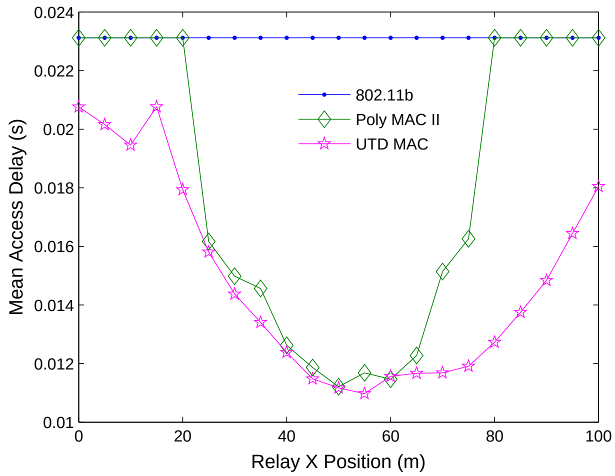

Fig. 12. Expected access delay vs. R's position along the S-D axis, S-D distance is 100 m

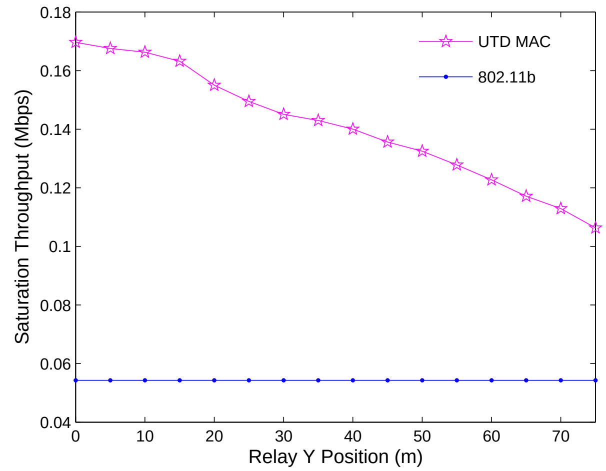

Fig. 13. Throughput vs. R's position orthogonal to the S-D axis, S-D distance is 150 m

TABLE III
BIT RATE PAIRS FOR UTD MAC IN FIGS. 13 AND 14

R's Y position from S-D axis (m)	0-20	25-30	35-75
S Rate (Mbps)	2	2	1
R Rate (Mbps)	2	1	1

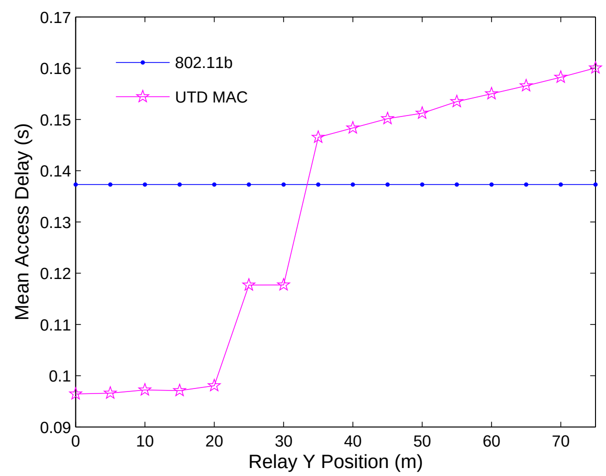

Fig. 14. Expected Access delay vs. R's position orthogonal to the S-D axis, S-D distance is 150 m

is 100 m. R position varies along the S-D axis. S and D coordinates are $(0, 0)$ and $(100, 0)$ respectively. R coordinates are $(X, 0)$, where X is the value on the horizontal axis in both figures. Traffic is one-way. The throughput of the cooperative protocols is significantly affected by the position of R. Poly MAC II does not invoke cooperation when $X \leq 20$ and $X \geq 80$ m. The UTD MAC curves consist of a sequence of segments, each segment being obtained with a specific pair of transmission rates for S and R respectively. The rate pairs are reported in Table II and help explain the UTD MAC plots. Sudden changes in the plots occur when the optimal transmission rate of either S or R changes. In the $0 \leq X \leq 10$ m region the transmission rate of both S and R is 1 Mbps, as both nodes attempt to reach D from approximately the same distance. In the $15 \leq X \leq 35$ m region, however, R increases its rate to 2 Mbps, thus providing a faster frame transmission time. In turn, S changes to 11 Mbps as it provides the fastest solution to send the frame to R. In the $65 \leq X \leq 100$ m region R increasingly approaches D. S rate goes down to 2 Mbps, which is a suitable rate to reach both R and D. When only R is reached successfully by the frame, R rate of 11 Mbps delivers the frame to D at full speed, taking advantage of the reduced distance to D.

Figs. 13 and 14 shows throughput and expected access delay respectively, under saturation load when the S-D distance is 150 m. R position varies orthogonal to the S-D axis. S and D coordinates are $(0, 0)$ and $(150, 0)$ respectively. R coordinates are $(75, Y)$, where Y is the value on the horizontal axis in both figures. Traffic is two-way. In this scenario, Poly MAC II never invokes cooperation. Only IEEE 802.11b and UTD MAC are shown then. Even when R is 75 m away from the S-D axis, the cooperative protocol yields a noticeable throughput gain over IEEE 802.11b. The behavior of the access delay curve for UTD MAC as Y increases can be explained by inspecting the transmission rates used by S and R (Table III). The step like delay increase in the $20 \leq Y \leq 30$ m region occurs due to the rate reduction from 1 to 2 Mbps performed by R first, then by S. It must be noted that R rate is decreased before S rate is, as R must ensure reliable delivery to D, whereas S can be more aggressive given that R can provide a backup transmission attempt. In the $35 \leq Y \leq 75$ m region the access delay increases slightly and it exceeds the delay of IEEE 802.11. This is because all nodes use 1 Mbps and the transmission via R takes longer time than the direct transmission from S to D.

Overall, both cooperative protocols offer tangible performance gains when compared to IEEE 802.11b if R is conveniently located between S and D. UTD MAC appears to be somewhat more flexible in accommodating the various positions of R.

A. *Performance of IEEE 802.11b*

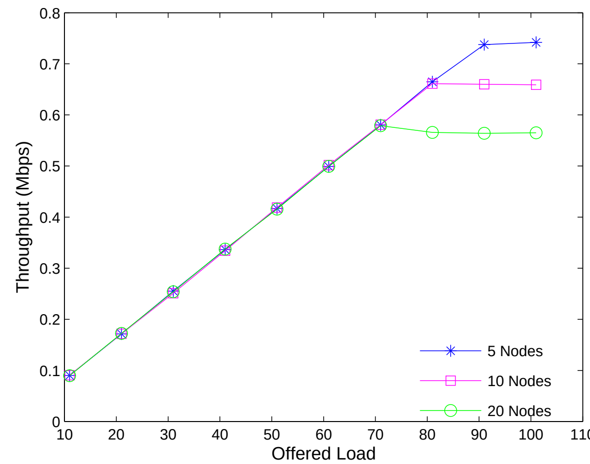

Fig. 15. Throughput vs. Arrival Rate, each node generates equal traffic, No frame error, transmission rate is 1 Mbps

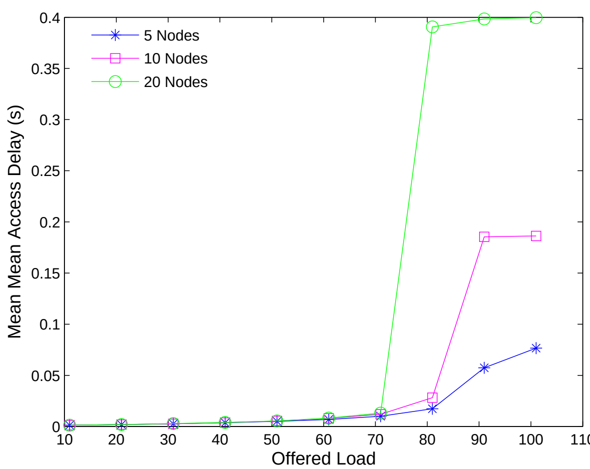

Fig. 16. Expected access delay vs. Arrival Rate, each node generates equal traffic, No frame error, transmission rate is 1 Mbps

Figs. 15, 16 and 17 shows throughput, expected access delay and expected number of retransmission attempts as a function of offered load and number of nodes for the IEEE 802.11b. The transmission rate for all nodes is 1 Mbps. As number of nodes increase, the throughput decreases due to collisions. The lowering of throughput is reflected as higher access delay. The number of retransmission attempts increases as number of nodes increases. The graphs have been plotted assuming no frame error which is an ideal case.

Figs. 18, 19 and 20 show throughput, expected access delay and expected number of retransmission attempts as a function of offered load and number of nodes for the IEEE 802.11b. The transmission rate for all nodes is 2 Mbps. As compared to the throughput attained using a rate of 1 Mbps, the throughput obtained using 2 Mbps is greater. The assumption that there are no frame errors is applicable in these figures too.

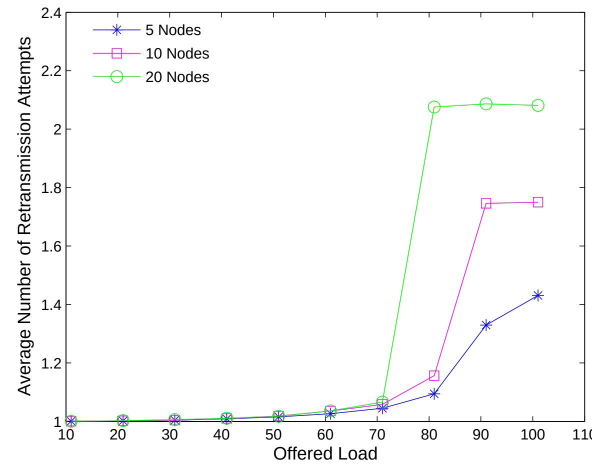

Fig. 17. Expected retransmission attempt vs. Arrival Rate, each node generates equal traffic,No frame error, transmission rate is 1 Mbps

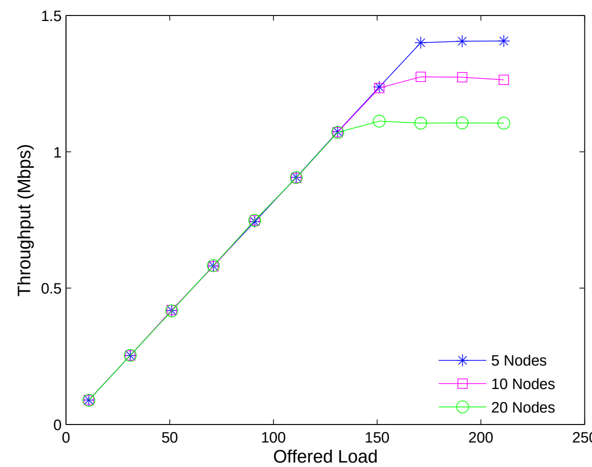

Fig. 18. Throughput vs. Arrival Rate, each node generates equal traffic, No frame error, transmission rate is 2 Mbps

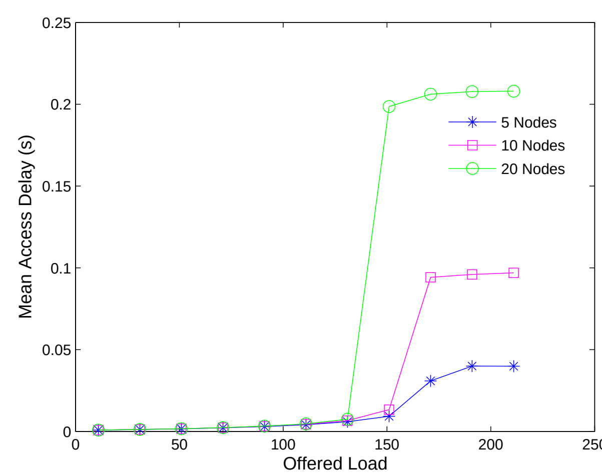

Fig. 19. Expected access delay vs. Arrival Rate, each node generates equal traffic,No frame error, transmission rate is 2 Mbps

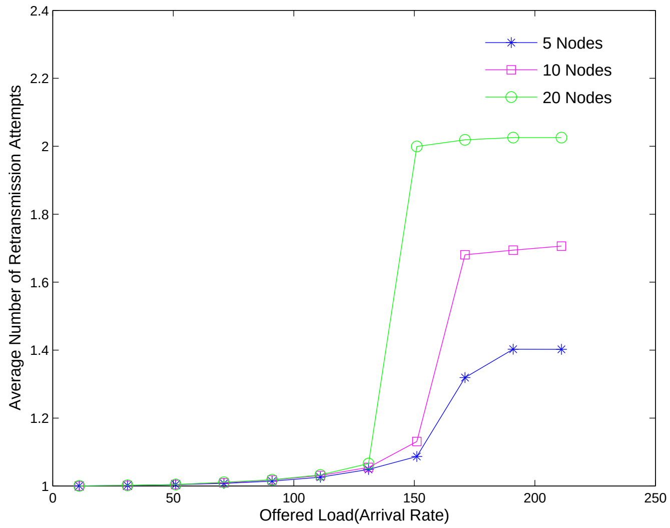

Fig. 20. Expected retransmission attempt vs. Arrival Rate, each node generates equal traffic, No frame error, transmission rate is 2 Mbps

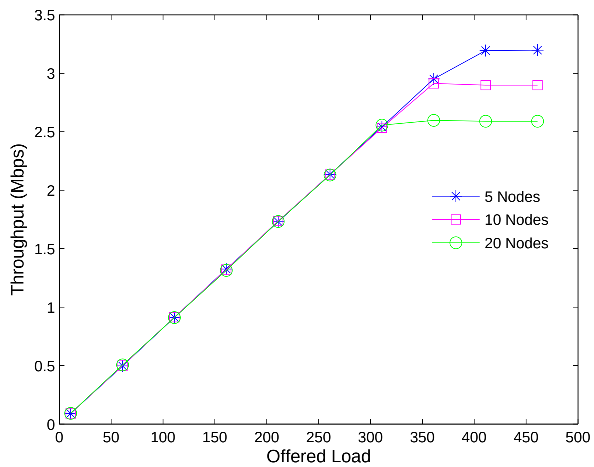

Fig. 21. Throughput vs. Arrival Rate, each node generates equal traffic, No frame error, transmission rate is 5.5 Mbps

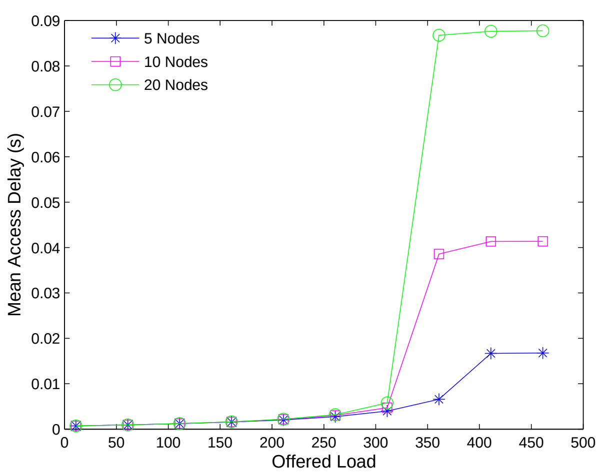

Fig. 22. Expected access delay vs. Arrival Rate, each node generates equal traffic,No frame error, transmission rate is 5.5 Mbps

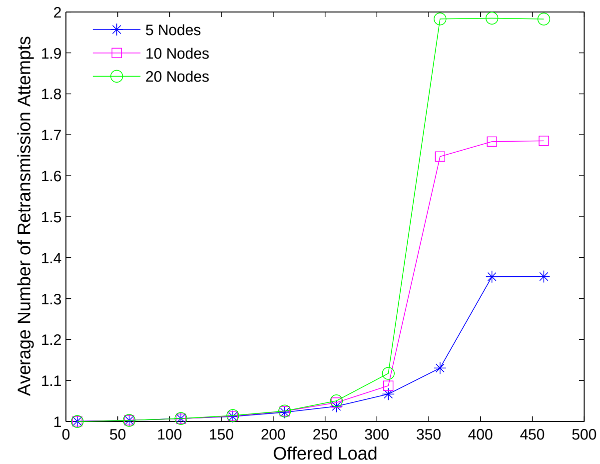

Fig. 23. Expected retransmission attempt vs. Arrival Rate, each node generates equal traffic,No frame error, transmission rate is 5.5 Mbps

Figs. 21, 22 and 23 show throughput, expected access delay and expected number of retransmission attempts as a function of offered load and number of nodes for the IEEE 802.11b. A transmission rate of 5.5 Mbps is used by all the nodes) As compared to the throughput attained using a rate of 1 Mbps and 2 Mbps, the throughput obtained using 5.5 Mbps is greater.Again, it is assumed that there are no frame errors.

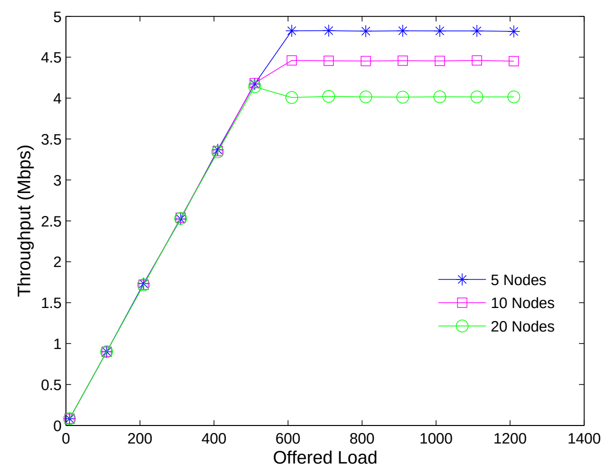

Fig. 24. Throughput vs. Arrival Rate, each node generates equal traffic, No frame error, transmission rate is 11 Mbps

Figs. 24, 25 and 26 show throughput, expected access delay and expected number of retransmission attempts as a function of offered load and number of nodes for the IEEE 802.11b. The transmission rate for all nodes is 11 Mbps. The plots show that, the throughput obtained using 11 Mbps is higher than the throughput achieved using 1, 2 and 5.5 Mbps. It is assumed that there are no frame errors.

B. UTD Cooperative Protocol Results - 1 Mbps

Figs. 27, 28 and 29 show the saturation throughput, expected access delay and expected number of retransmission

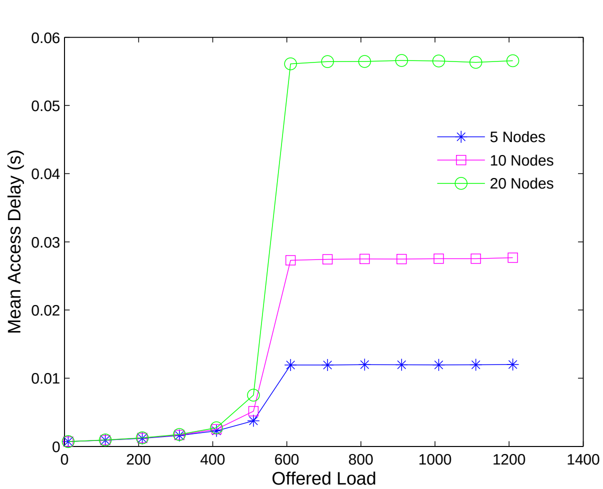

Fig. 25. Expected access delay vs. Arrival Rate, each node generates equal traffic,No frame error, transmission rate is 11 Mbps

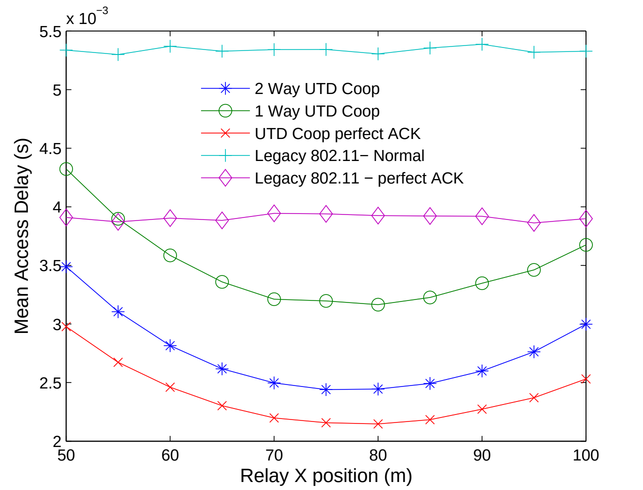

Fig. 28. Expected access delay vs. R's position along the S-D axis, S-D distance is 50 m, transmission rate is 1 Mbps

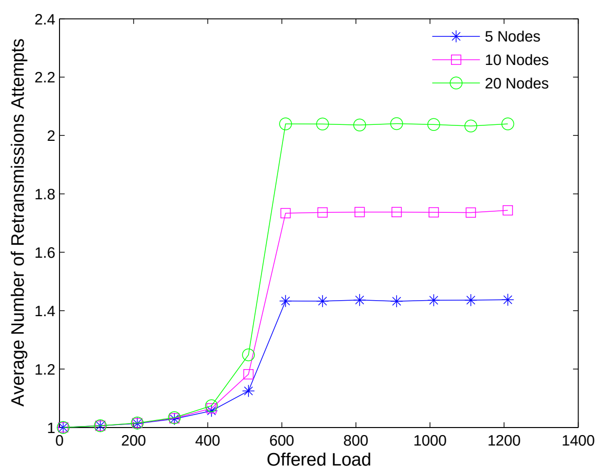

Fig. 26. Expected retransmission attempt vs. Arrival Rate, each node generates equal traffic,No frame error, transmission rate is 11 Mbps

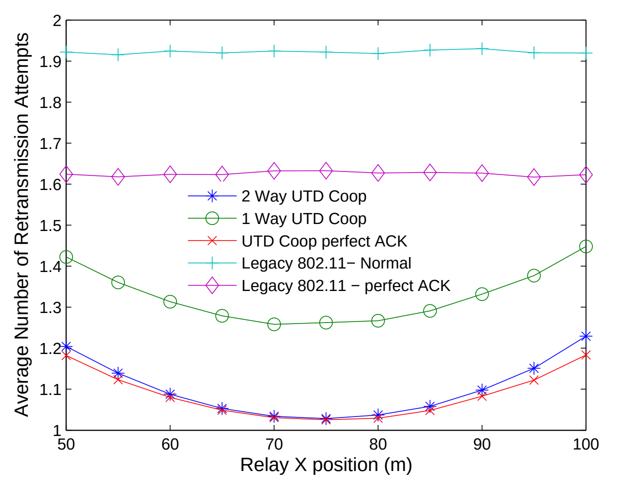

Fig. 29. Expected retransmission attempts vs. R's position along the S-D axis, S-D distance is 50 m, transmission rate is 1 Mbps

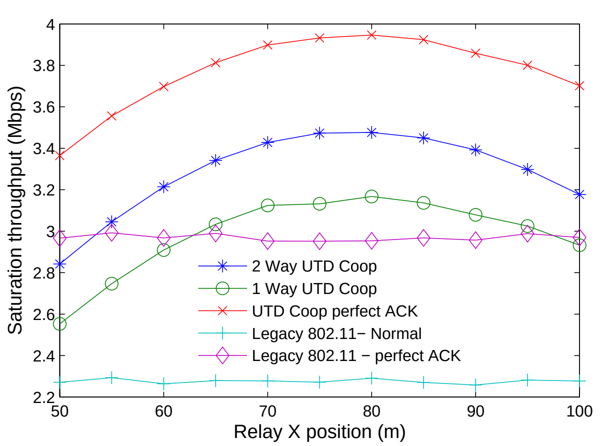

Fig. 27. Throughput vs. R's position along the S-D axis, S-D distance is 50 m, transmission rate is 1 Mbps

attempts for the different flavors of IEEE 802.11b and UTD MAC when the S-D distance is 50 m. S is at $(50, 0)$, D is at $(100, 0)$ and R is at $(X, 0)$ where X varies between 50 and 150 m. The transmission rate for all three nodes is 1 Mbps. When ACK is perfect (without errors), the throughput increases significantly. This shows that the ACKs have to be handled carefully. If ACKs are made reliable, the throughput can be improved significantly. The increase in throughput is correlated to the decrease in access delay. For comparison, the expected number of retransmission attempts for each case are shown. The graph also shows that UTD MAC with cooperation enabled for ACK frame transfer (2-Way UTD coop) has a significant throughput increase when compared to one way UTD MAC protocol. When R is very close to S, cooperation becomes an overhead. In this case, S has feeble chance of delivering the frame to D. When S fails, R which is also far from D cannot really help. R fails to deliver the frame most of the times. When ACK is also cooperated, R has feeble chance of receiving the frame from D. Hence R cannot help much. This results in wastage of channel time and hence throughput is less compared to legacy 802.11b with perfect ACK.

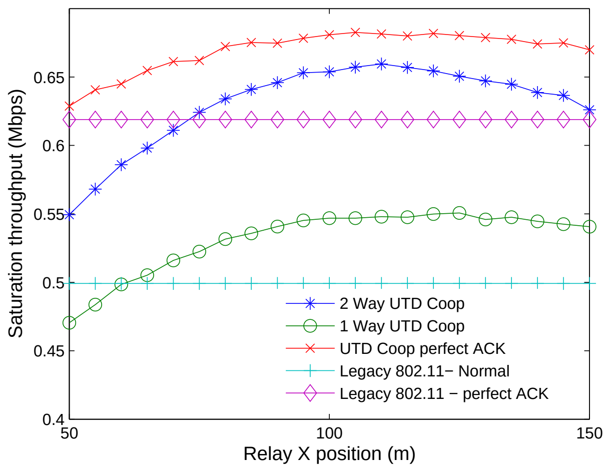

Fig. 30. Throughput vs. R's position along the S-D axis, S-D distance is 100 m, transmission rate is 1 Mbps

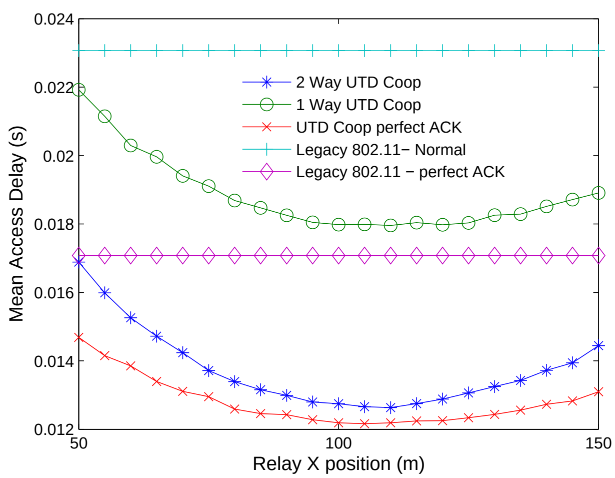

Fig. 31. Expected access delay vs. R's position along the S-D axis, S-D distance is 100 m, transmission rate is 1 Mbps

Figs. 30, 31 and 32 show throughput, expected access delay and the expected number of retransmission attempts under saturation load when the S-D distance is 100 m. R position varies along the S-D axis. S and D coordinates are $(50, 0)$ and $(150, 0)$ respectively. R coordinates are $(X, 0)$, where X is the value on the horizontal axis in both figures. Traffic is one-way and the transmission rate is 1 Mbps for all traffic between S, R and D. The throughput of the cooperative protocols is significantly affected by the ACK packets delivery. We notice that UTD MAC with perfect ACK feature achieves the maximum throughput.

Figs. 33, 34 and 35 show throughput, expected access delay and expected number of retransmission attempts under saturation load when the S-D distance is 150 m. R position varies along the S-D axis. S and D coordinates are $(50, 0)$

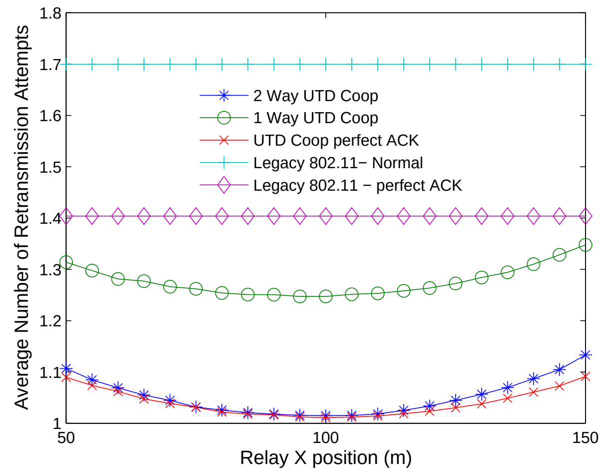

Fig. 32. Expected retransmission attempt vs. R's position along the S-D axis, S-D distance is 100 m, transmission rate is 1 Mbps

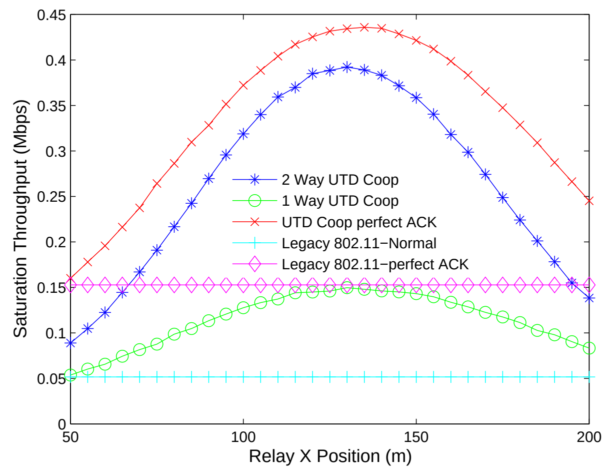

Fig. 33. Throughput vs. R's position along the S-D axis, S-D distance is 150 m, transmission rate is 1 Mbps

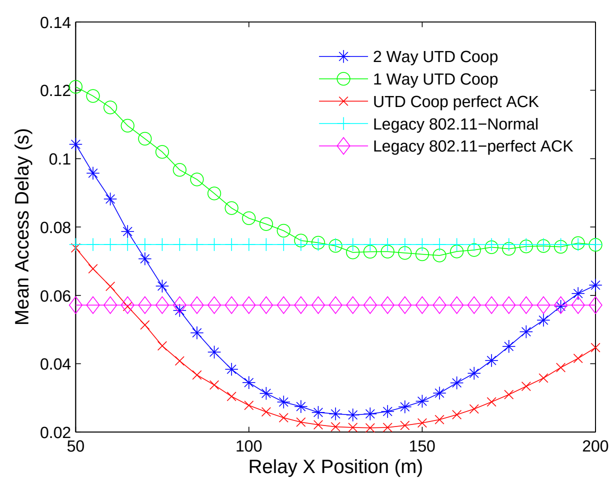

Fig. 34. Expected access delay vs. R's position along the S-D axis, S-D distance is 150 m, transmission rate is 1 Mbps

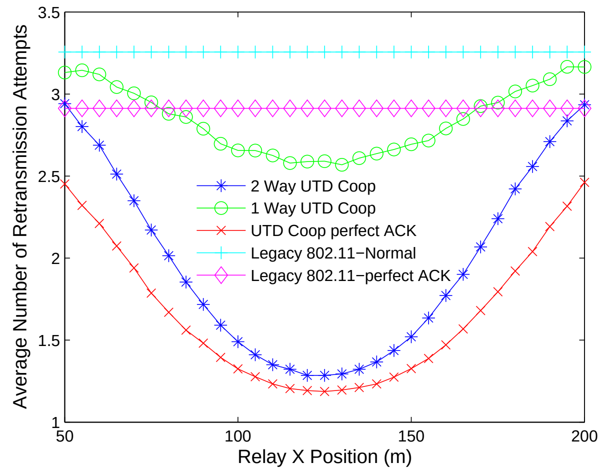

Fig. 35. Expected retransmission attempt vs. R's position along the S-D axis, S-D distance is 150 m, transmission rate is 1 Mbps

and $(200, 0)$ respectively. R coordinates are $(X, 0)$, where X is the value on the horizontal axis in both figures. Traffic is one-way and the transmission rate is 1 Mbps for all traffic between S, R and D.

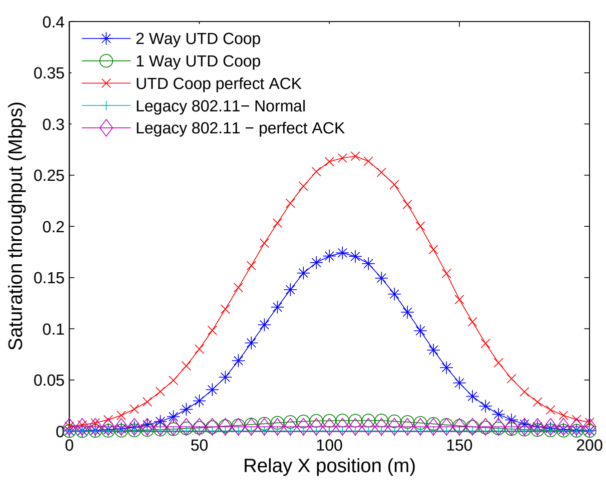

Fig. 36. Throughput vs. R's position along the S-D axis, S-D distance is 200 m, transmission rate is 1 Mbps

Figs. 36, 37 and 38 show saturation throughput, expected access delay and the expected retransmission attempts when the S-D distance is 200 m. R position varies along the S-D axis. S and D coordinates are $(0, 0)$ and $(200, 0)$ respectively. R coordinates are $(X, 0)$, where X is the value on the horizontal axis in the figures. Traffic is one-way and the transmission rate is 1 Mbps for all traffic between S, R and D. For very large distances between S and D, for e.g., 200m, cooperation on data frames alone does not help improve the throughput. Two way cooperation i.e.,cooperation for both data and ACK frames provide a drastic increase in throughput.

Figs. 39, 40 and 41 show saturation throughput, expected access delay and expected number of retransmission attempts when the S-D distance is 50 m. R position varies along

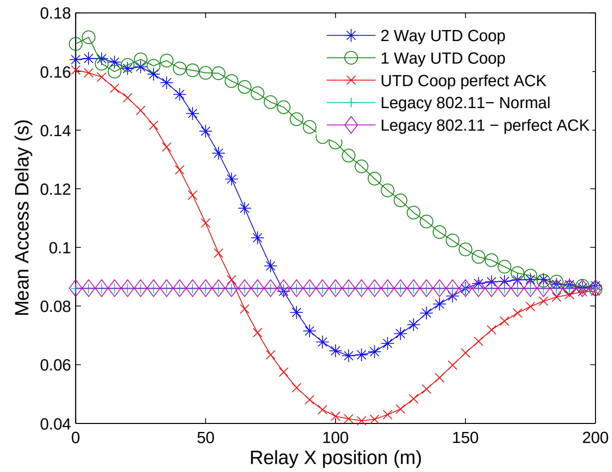

Fig. 37. Expected access delay vs. R's position along the S-D axis, S-D distance is 200 m, transmission rate is 1 Mbps

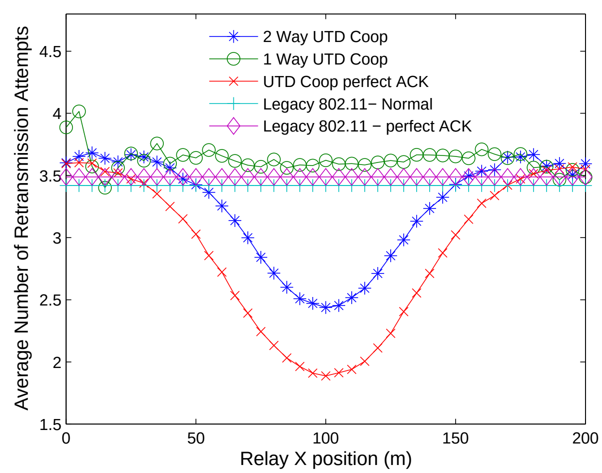

Fig. 38. Expected retransmission attempt vs. R's position along the S-D axis, S-D distance is 200 m, transmission rate is 1 Mbps

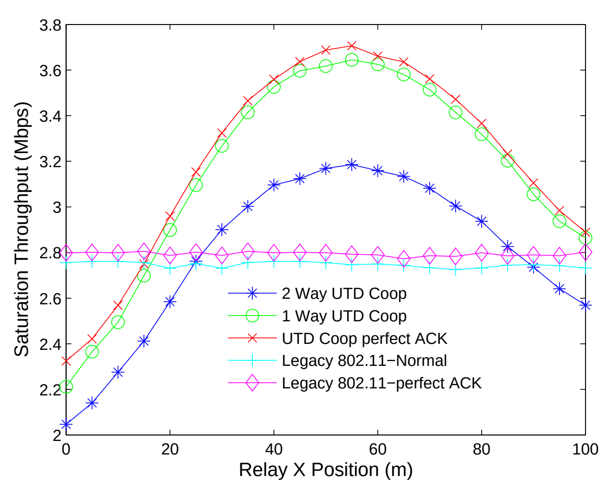

Fig. 39. Throughput vs. R's position along the S-D axis, S-D distance is 50 m, transmission rate is 1 Mbps

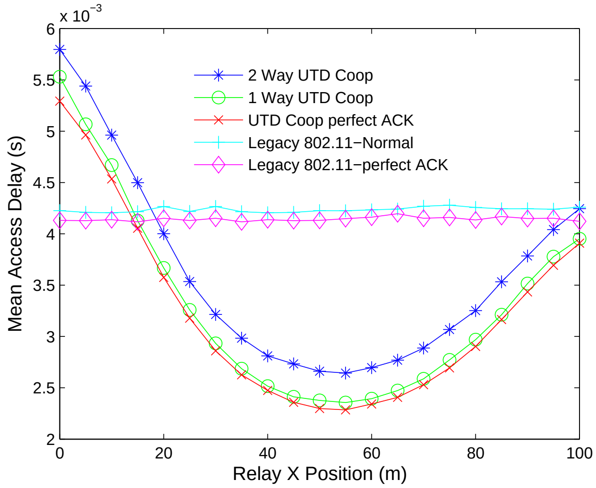

Fig. 40. Expected access delay vs. R's position along the S-D axis, S-D distance is 50 m, transmission rate is 1 Mbps

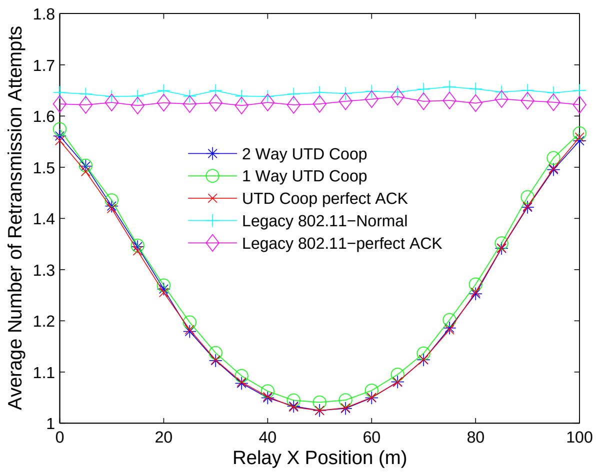

Fig. 41. Expected retransmission attempt vs. R's position along the S-D axis, S-D distance is 50 m, transmission rate is 1 Mbps

the S-D axis S and D coordinates are $(25, 0)$ and $(75, 0)$ respectively. R coordinates are $(X, 0)$, where X is the value on the horizontal axis in both figures. Traffic is one-way and the transmission rate is 1 Mbps for all traffic between S, R and D. R to the left of S or to the right of D does not help in improving the throughput. It is seen that the position of R is vital if we need throughput improvements.

Figs. 42, 43 and 44 show saturation throughput, expected access delay and expected number of retransmission attempts when the S-D distance is 100 m. R position varies along the S-D axis S and D coordinates are $(25, 0)$ and $(125, 0)$ respectively. R coordinates are $(X, 0)$, where X is the value on the horizontal axis in both figures. Traffic is one-way and the transmission rate is 1 Mbps for all traffic between S, R and D. It is reaffirmed that the position of R is vital for throughput improvements.

Figs. 45, 46 and 47 show saturation throughput, expected access delay and expected number of retransmission attempts when the S-D distance is 150 m. R position varies along

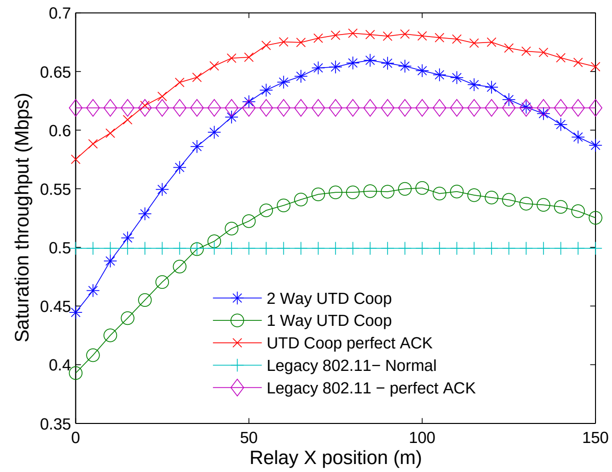

Fig. 42. Throughput vs. R's position along the S-D axis, S-D distance is 100 m, transmission rate is 1 Mbps

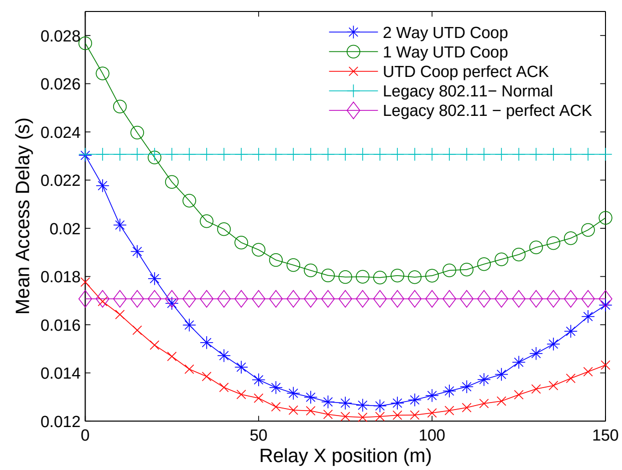

Fig. 43. Expected access delay vs. R's position along the S-D axis, S-D distance is 100 m, transmission rate is 1 Mbps

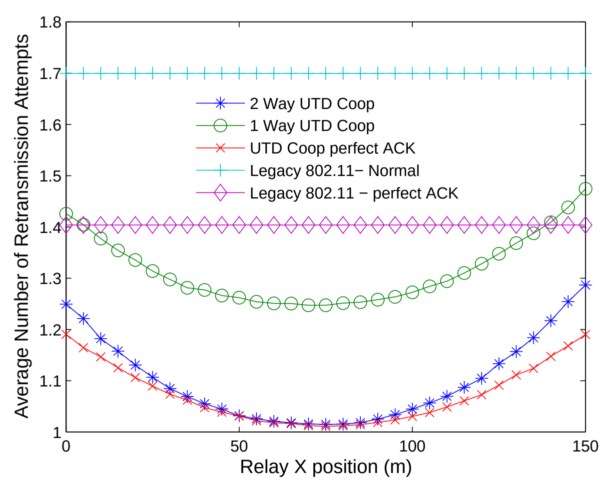

Fig. 44. Expected retransmission attempt vs. R's position along the S-D axis, S-D distance is 100 m, transmission rate is 1 Mbps

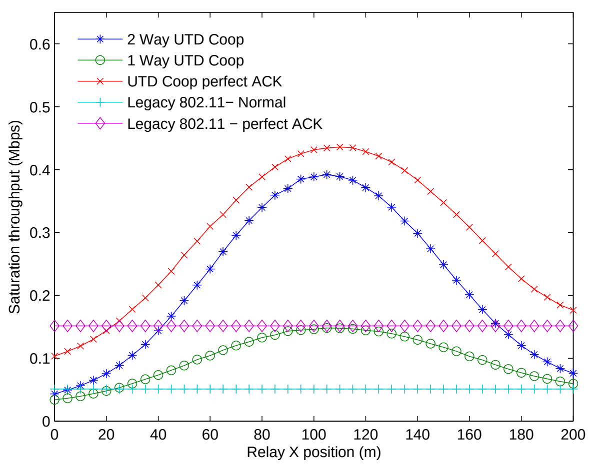

Fig. 45. Throughput vs. R's position along the S-D axis, S-D distance is 150 m, transmission rate is 1 Mbps

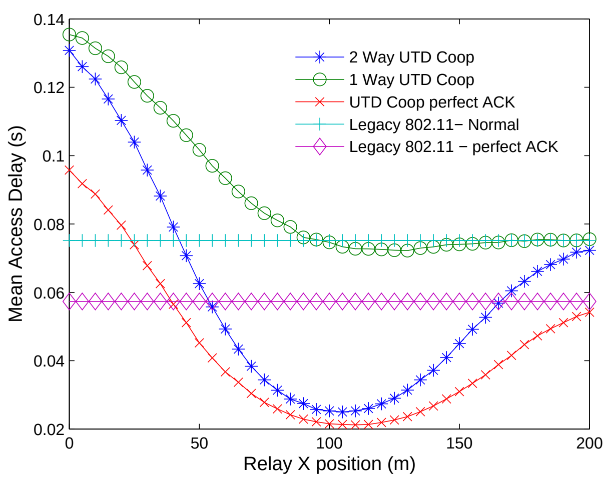

Fig. 46. Expected access delay vs. R's position along the S-D axis, S-D distance is 150 m, transmission rate is 1 Mbps

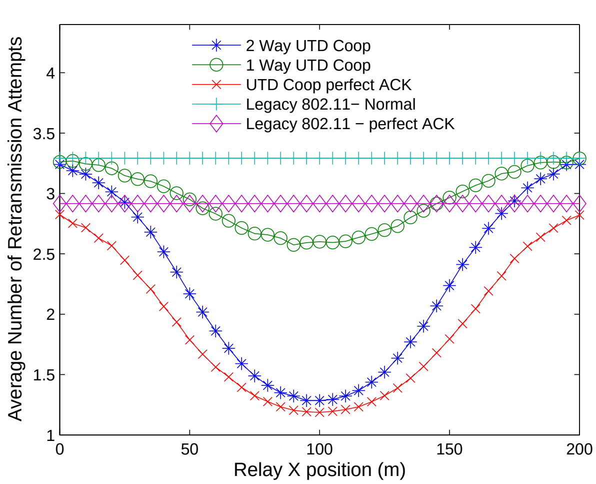

Fig. 47. Expected retransmission attempt vs. R's position along the S-D axis, S-D distance is 150 m, transmission rate is 1 Mbps

the S-D axis S and D coordinates are $(25, 0)$ and $(175, 0)$ respectively. R coordinates are $(X, 0)$, where X is the value on the horizontal axis in both figures. Traffic is one-way and the transmission rate is 1 Mbps for all traffic between S, R and D.

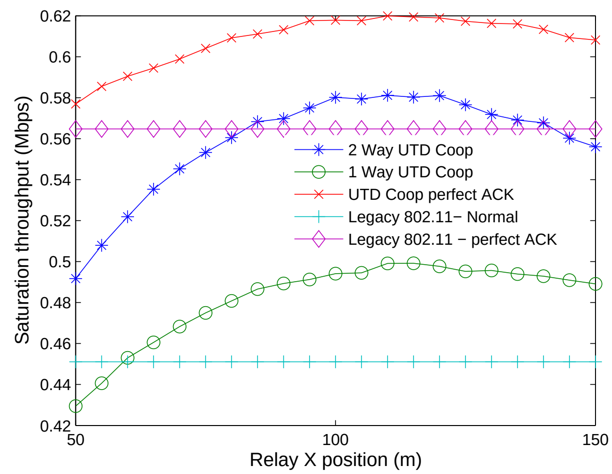

Fig. 48. Throughput vs. R's position along the S-D axis, S-D distance is 100 m, transmission rate is 1 Mbps, MAC payload size is 512 Bytes

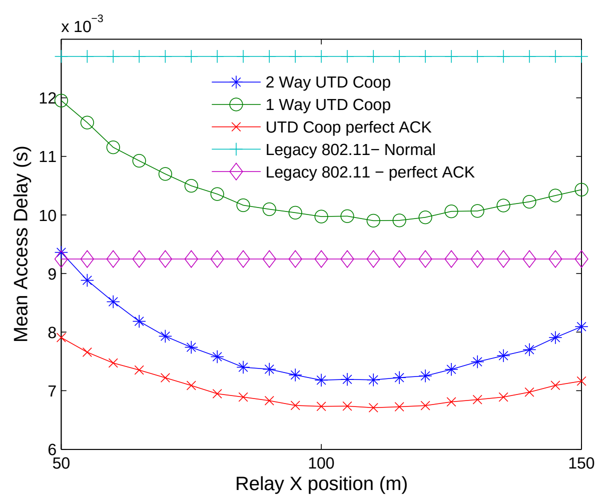

Fig. 49. Expected access delay vs. R's position along the S-D axis, S-D distance is 100 m, transmission rate is 1 Mbps, MAC payload size is 512 Bytes

The effect of packet length on throughput is studied. Figs. 48, 49 and 50 show saturation throughput, expected access delay and expected number of retransmission attempts when the S-D distance is 100 m. R position varies along the S-D axis. S and D coordinates are $(50, 0)$ and $(150, 0)$ respectively. R coordinates are $(X, 0)$, where X is the value on the horizontal axis in both figures. Traffic is one-way and the transmission rate is 1 Mbps for all traffic between S, R and D. The packet length is fixed at 512 bytes.

Figs. 51, 52 and 53 show saturation throughput, expected access delay and expected number of retransmission attempts when the S-D distance is 100 m. R position varies along

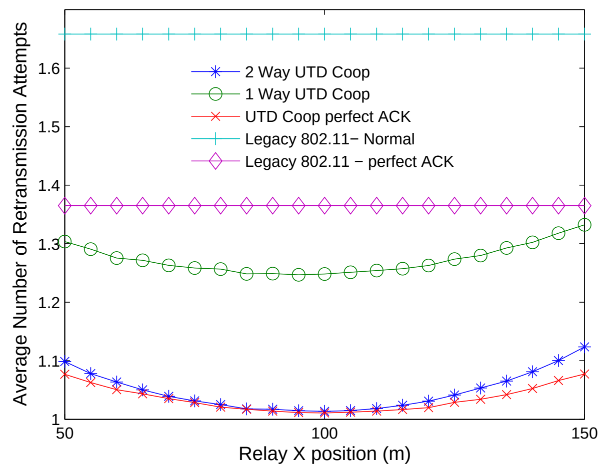

Fig. 50. Expected retransmission attempt vs. R's position along the S-D axis, S-D distance is 100 m, transmission rate is 1 Mbps, MAC payload size is 512 Bytes

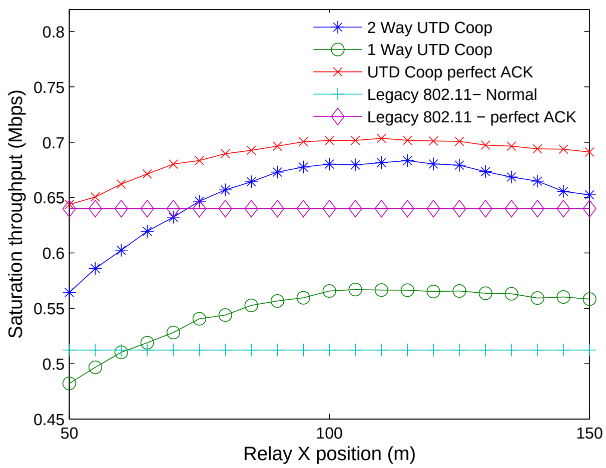

Fig. 51. Throughput vs. R's position along the S-D axis, S-D distance is 100 m, transmission rate is 1 Mbps, MAC payload size is 1500 Bytes

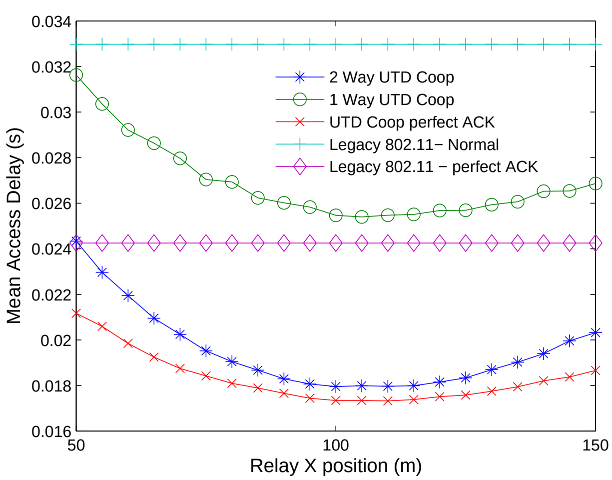

Fig. 52. Expected access delay vs. R's position along the S-D axis, S-D distance is 100 m, transmission rate is 1 Mbps, MAC payload size is 1500 Bytes

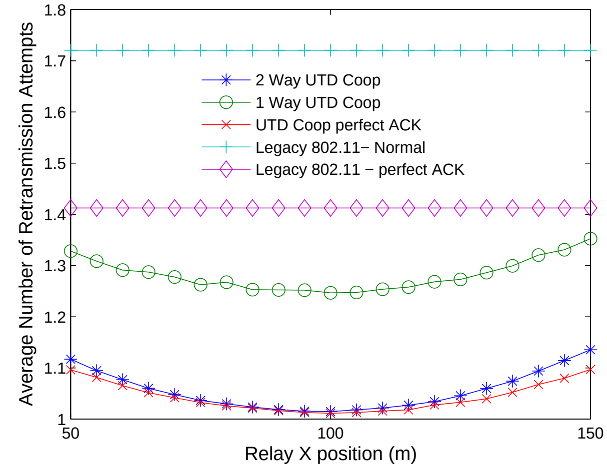

Fig. 53. Expected retransmission attempt vs. R's position along the S-D axis, S-D distance is 100 m, transmission rate is 1 Mbps, MAC payload size is 1500 Bytes

the S-D axis S and D coordinates are $(50, 0)$ and $(150, 0)$ respectively. R coordinates are $(X, 0)$, where X is the value on the horizontal axis in both figures. Traffic is one-way and the transmission rate is 1 Mbps for all traffic between S, R and D. The packet length is fixed at 1500 bytes. The throughput in this case is higher than the throughput with a packet size of 512 bytes.

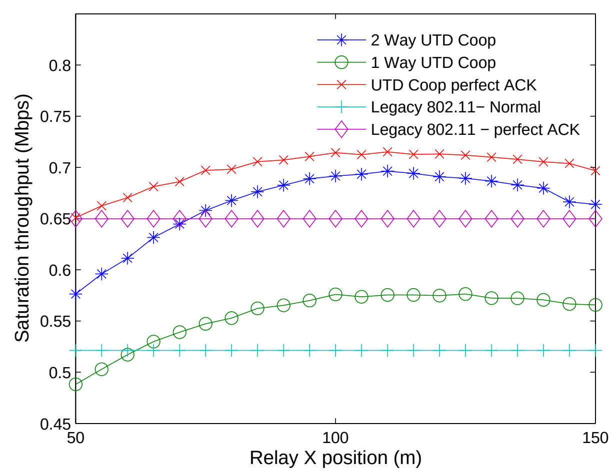

Fig. 54. Throughput vs. R's position along the S-D axis, S-D distance is 100 m, transmission rate is 1 Mbps, MAC payload size is 2048 Bytes

Figs. 54, 55 and 56 show saturation throughput, expected access delay and expected number of retransmission attempts when the S-D distance is 100 m. R position varies along the S-D axis S and D coordinates are $(50, 0)$ and $(150, 0)$ respectively. R coordinates are $(X, 0)$, where X is the value on the horizontal axis in both figures. Traffic is one-way and the transmission rate is 1 Mbps for all traffic between S, R and D. The packet length is fixed at 2048 bytes. The throughput in this case is higher than the throughput obtained when a packet size of 512 bytes or 1500 bytes is used. Thus an increase in

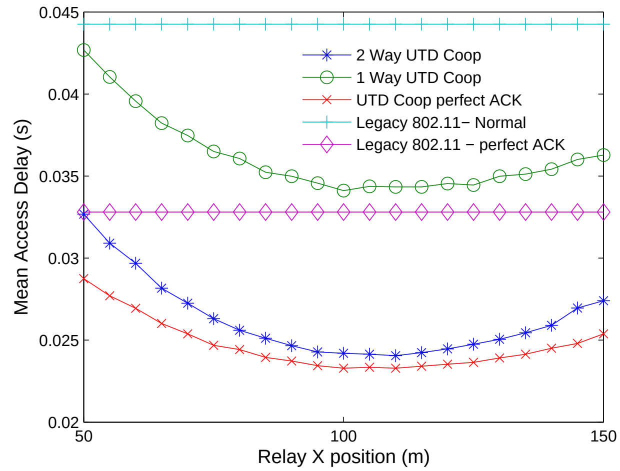

Fig. 55. Expected access delay vs. R's position along the S-D axis, S-D distance is 100 m, transmission rate is 1 Mbps, MAC payload size is 2048 Bytes

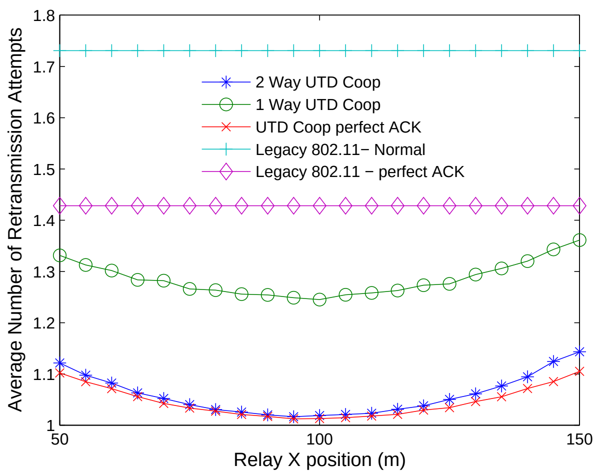

Fig. 56. Expected retransmission attempt vs. R's position along the S-D axis, S-D distance is 100 m, transmission rate is 1 Mbps, MAC payload size is 2048 Bytes

packet size increases the throughput obtained.

Figs. 57, 58 and 59 show saturation throughput, expected access delay and the expected retransmission attempts when the S-D distance is 50 m. R position varies along the S-D axis. S and D coordinates are $(50, 0)$ and $(100, 0)$ respectively. R coordinates are $(X, 0)$, where X is the value on the horizontal axis in both figures. Traffic is two-way and a fixed transmission rate of 1 Mbps for all traffic between S, R and D.

Figs. 60, 61 and 62 show saturation throughput, expected access delay and the expected retransmission attempts when the S-D distance is 100 m. R position varies along the S-D axis. S and D coordinates are $(50, 0)$ and $(150, 0)$ respectively. R coordinates are $(X, 0)$, where X is the value on the horizontal axis in both figures. Traffic is two-way and a fixed transmission rate of 1 Mbps for all traffic between S, R and D.

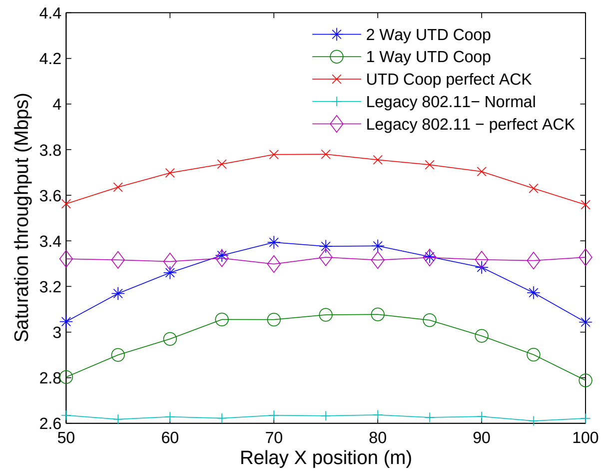

Fig. 57. Throughput vs. R's position along the S-D axis, S-D distance is 50 m, transmission rate is 1 Mbps, 2-way traffic

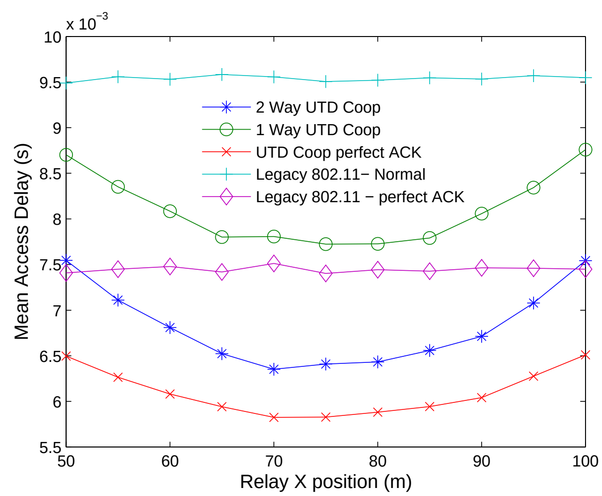

Fig. 58. Expected access delay vs. R's position along the S-D axis, S-D distance is 50 m, transmission rate is 1 Mbps, 2-way traffic

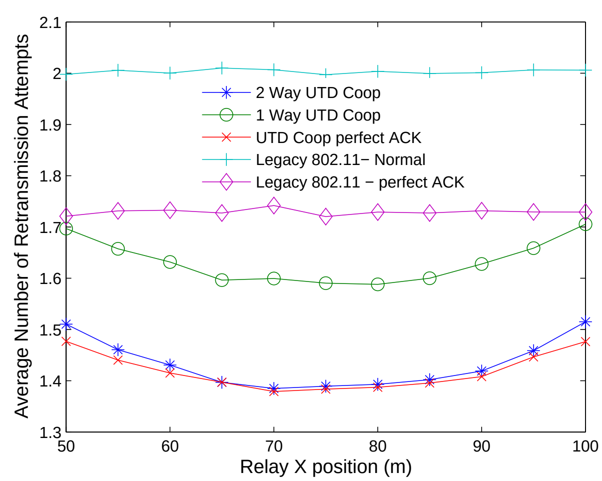

Fig. 59. Expected retransmission attempt vs. R's position along the S-D axis, S-D distance is 50 m, transmission rate is 1 Mbps, 2-way traffic

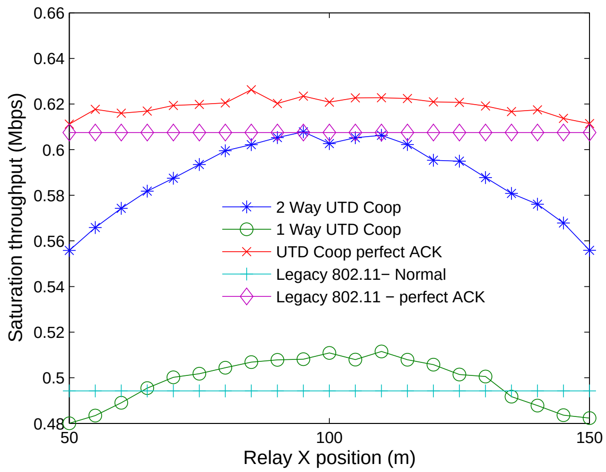

Fig. 60. Throughput vs. R's position along the S-D axis, S-D distance is 100 m, transmission rate is 1 Mbps, 2-way traffic

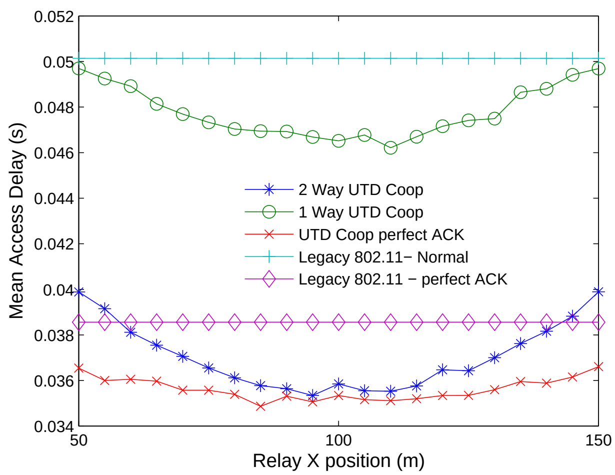

Fig. 61. Expected access delay vs. R's position along the S-D axis, S-D distance is 100 m, transmission rate is 1 Mbps, 2-way traffic

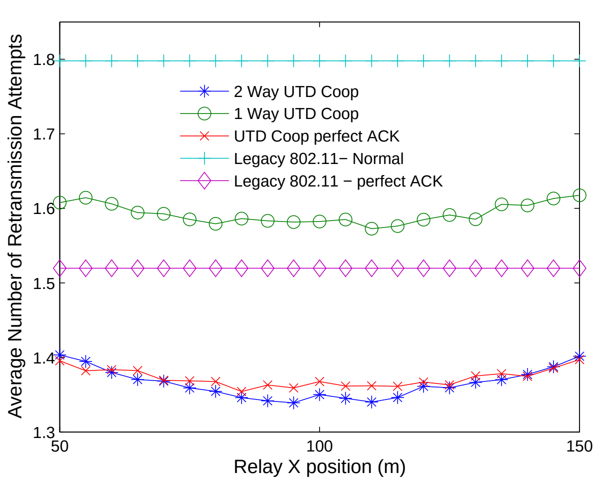

Fig. 62. Expected retransmission attempt vs. R's position along the S-D axis, S-D distance is 100 m, transmission rate is 1 Mbps, 2-way traffic

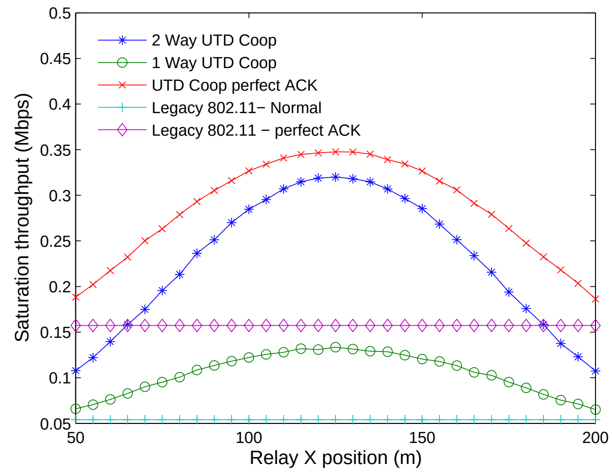

Fig. 63. Throughput vs. R's position along the S-D axis, S-D distance is 150 m, transmission rate is 1 Mbps, 2-way traffic

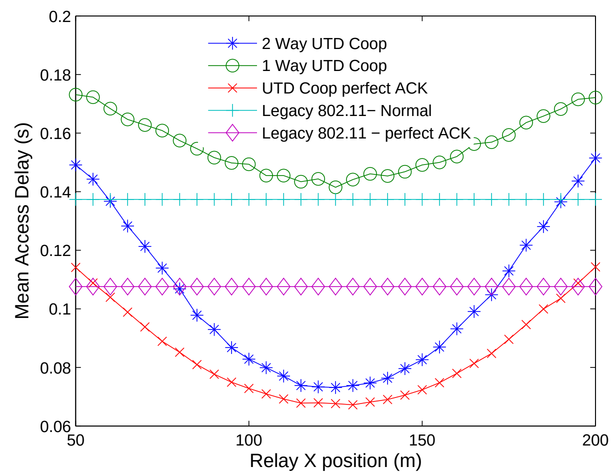

Fig. 64. Expected access delay vs. R's position along the S-D axis, S-D distance is 150 m, transmission rate is 1 Mbps, 2-way traffic

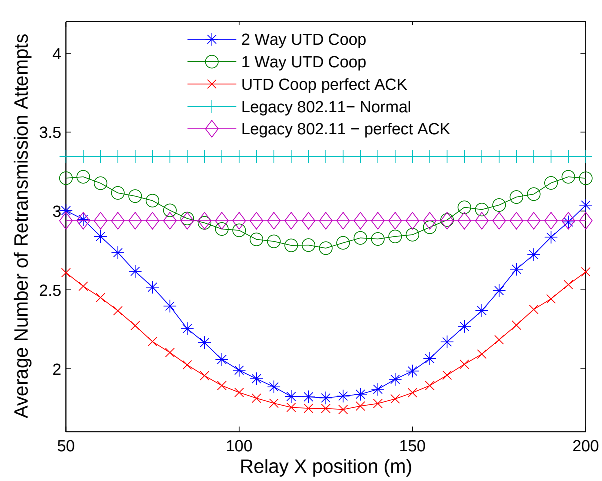

Fig. 65. Expected retransmission attempt vs. R's position along the S-D axis, S-D distance is 150 m, transmission rate is 1 Mbps, 2-way traffic

Figs. 63, 64 and 65 show throughput, expected access delay and the expected number of retransmission attempts, respectively under saturation load when the S-D distance is 150 m. R position varies along the S-D axis. S and D coordinates are $(50, 0)$ and $(200, 0)$ respectively. R coordinates are $(X, 0)$, where X is the value on the horizontal axis in both figures. Traffic is two-way and a fixed transmission rate of 1 Mbps for all traffic between S, R and D. As the distance between the source and the destination increases, two way cooperation becomes advantageous.

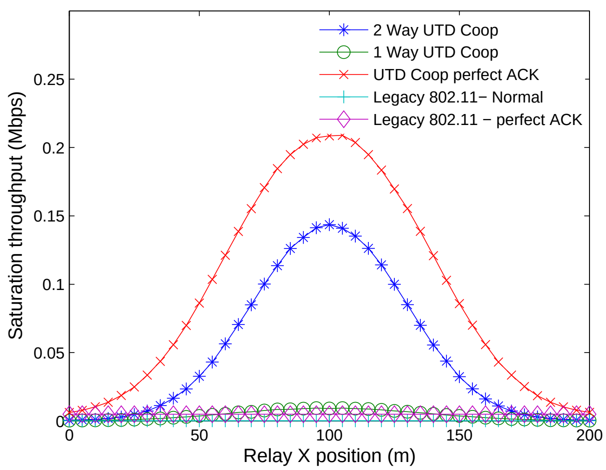

Fig. 66. Throughput vs. R's position along the S-D axis, S-D distance is 200 m, transmission rate is 1 Mbps, 2-way traffic

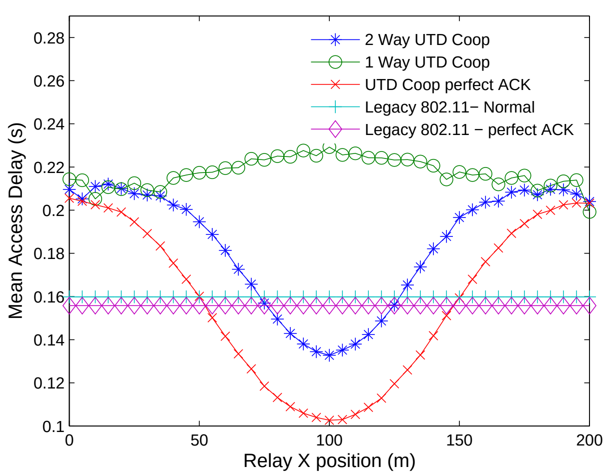

Fig. 67. Expected access delay vs. R's position along the S-D axis, S-D distance is 200 m, transmission rate is 1 Mbps, 2-way traffic

Figs. 66, 67 and 68 show throughput, expected access delay and the expected number of retransmission attempts respectively, under saturation load when the S-D distance is 200 m. R position varies along the S-D axis. S and D coordinates are $(0, 0)$ and $(200, 0)$ respectively. R coordinates are $(X, 0)$, where X is the value on the horizontal axis in both figures. Traffic is two-way and the a fixed transmission rate of 1 Mbps for all traffic between S, R and D. At very large distances between source and destination, cooperation for both data and ACK packets brings a significant improvement in throughput compared to IEEE 802.11b.

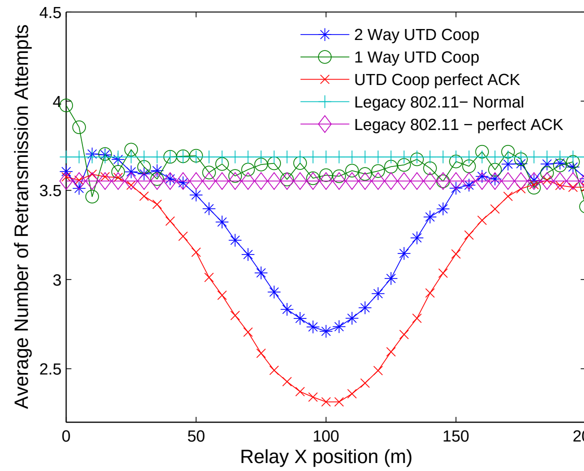

Fig. 68. Expected retransmission attempt vs. R's position along the S-D axis, S-D distance is 200 m, transmission rate is 1 Mbps, 2-way traffic

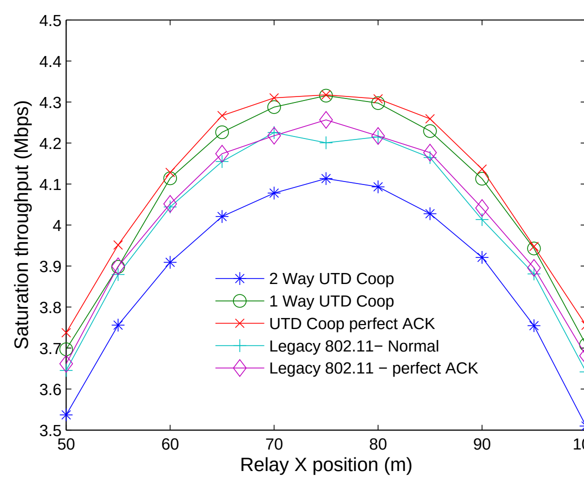

Fig. 69. Throughput vs. R's position along the S-D axis, S-D distance is 50 m, transmission rate is 1 Mbps, 3-way traffic

So far, the relay node was not generating any traffic. The effect of relay node generating traffic is studied. The traffic between R-S and R-D will not be cooperated i.e., these will be operating at IEEE 802.11b. Figs. 69, 70 and 71 show throughput, expected access delay and the expected number of retransmission attempts respectively under saturation load when the S-D distance is 50 m. R position varies along the S-D axis and also with and without the presence of perfect ACK. S and D coordinates are $(50, 0)$ and $(100, 0)$ respectively. R coordinates are $(X, 0)$, where X is the value on the horizontal axis in both figures. Traffic is three-way, i.e., all three nodes S, R and D generates traffic and a fixed transmission rate of 1 Mbps is used for all traffic between S, R and D. With R also adding its frames to the traffic, it is seen that two way cooperation becomes an overhead. Cooperation for data frames

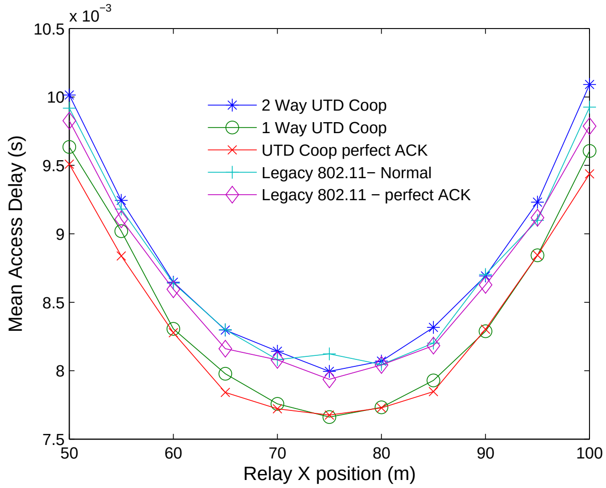

Fig. 70. Expected access delay vs. R's position along the S-D axis, S-D distance is 50 m, transmission rate is 1 Mbps, 3-way traffic

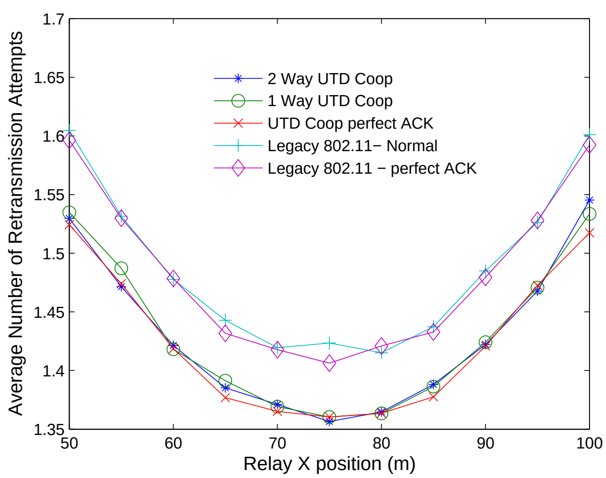

Fig. 71. Expected retransmission attempt vs. R's position along the S-D axis, S-D distance is 50 m, transmission rate is 1 Mbps, 3-way traffic

improves throughput.

Figs. 72, 73 and 74 show throughput, expected access delay and the expected number of retransmission attempts respectively, under saturation load when the S-D distance is 100 m. R position varies along the S-D axis and also with and without the presence of perfect ACK. S and D coordinates are $(50, 0)$ and $(150, 0)$ respectively. R coordinates are $(X, 0)$, where X is the value on the horizontal axis in both figures. Traffic is three-way, i.e., all three nodes S, R and D generates traffic and a fixed transmission rate of 1 Mbps is used for all traffic between S, R and D. When S and D are far apart, reliable ACKs improve throughput. Thus two way cooperation performs better than one way cooperation.

Figs. 75, 76 and 77 show throughput, expected access delay and the expected number of retransmission attempts respectively, under saturation load when the S-D distance is 150 m. R position varies along the S-D axis and also with and without the presence of perfect ACK. S and D coordinates are $(50, 0)$ and $(200, 0)$ respectively. R coordinates are $(X, 0)$,

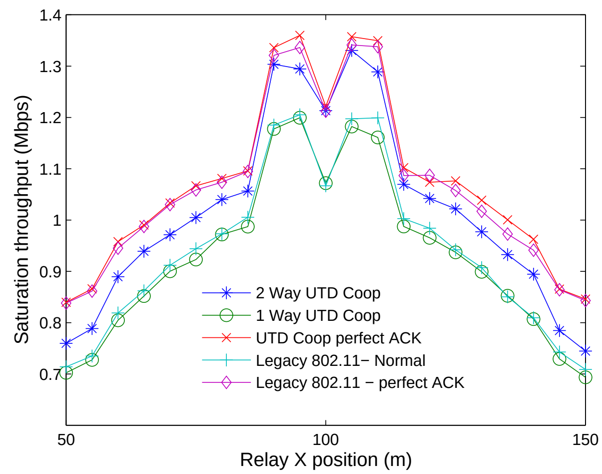

Fig. 72. Throughput vs. R's position along the S-D axis, S-D distance is 100 m, transmission rate is 1 Mbps, 3-way traffic

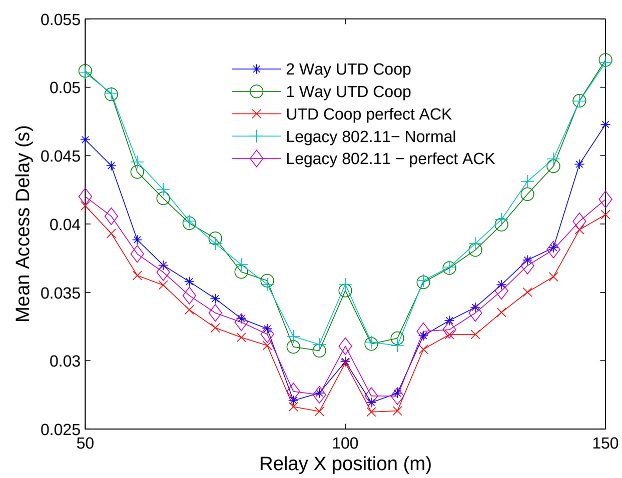

Fig. 73. Expected access delay vs. R's position along the S-D axis, S-D distance is 100 m, transmission rate is 1 Mbps, 3-way traffic

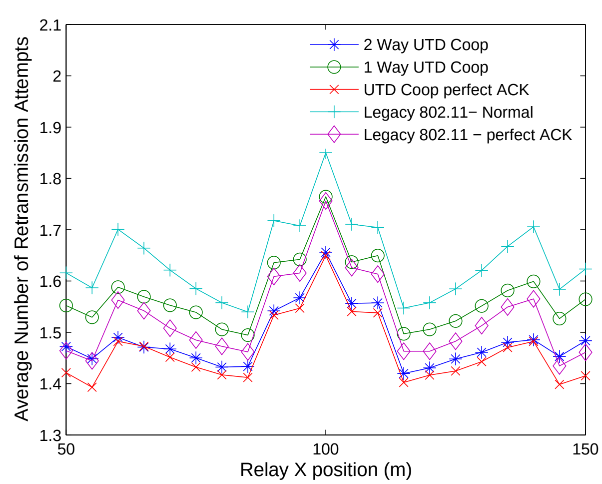

Fig. 74. Expected retransmission attempt vs. R's position along the S-D axis, S-D distance is 100 m, transmission rate is 1 Mbps, 3-way traffic

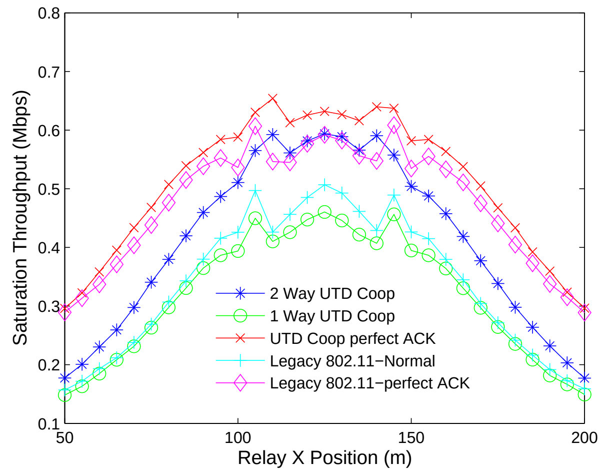

Fig. 75. Throughput vs. R's position along the S-D axis, S-D distance is 150 m, transmission rate is 1 Mbps, 3-way traffic

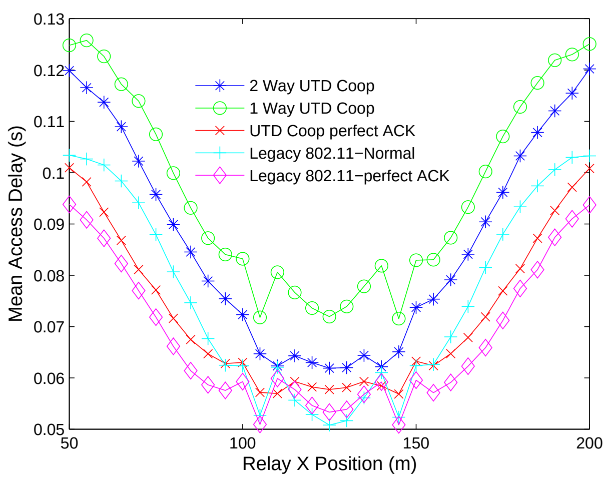

Fig. 76. Expected access delay vs. R's position along the S-D axis, S-D distance is 150 m, transmission rate is 1 Mbps, 3-way traffic

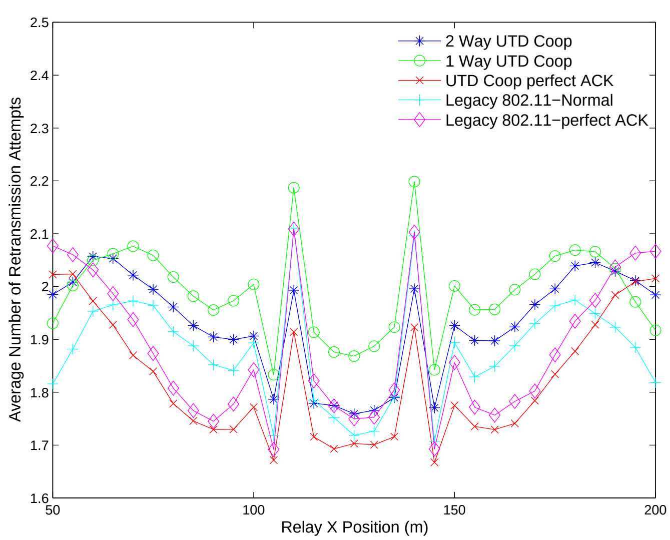

Fig. 77. Expected retransmission attempt vs. R's position along the S-D axis, S-D distance is 150 m, transmission rate is 1 Mbps, 3-way traffic

where X is the value on the horizontal axis in both figures. Traffic is three-way, i.e., all three nodes S, R and D generates traffic and a fixed transmission rate of 1 Mbps is used for all traffic between S, R and D. When S and D are far apart, reliable ACKs improve throughput. Thus two way cooperation performs better than one way cooperation.

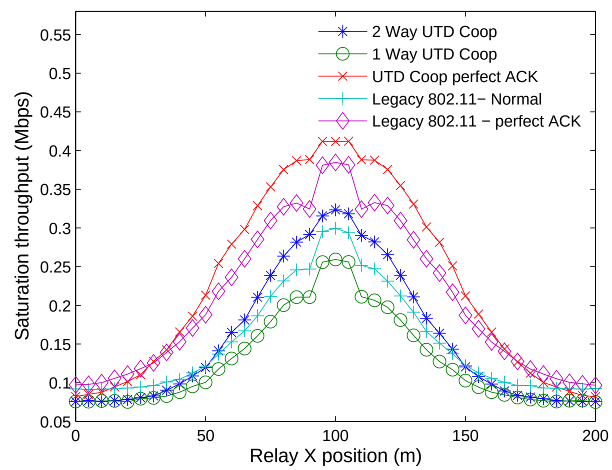

Fig. 78. Throughput vs. R's position along the S-D axis, S-D distance is 200 m, transmission rate is 1 Mbps, 3-way traffic

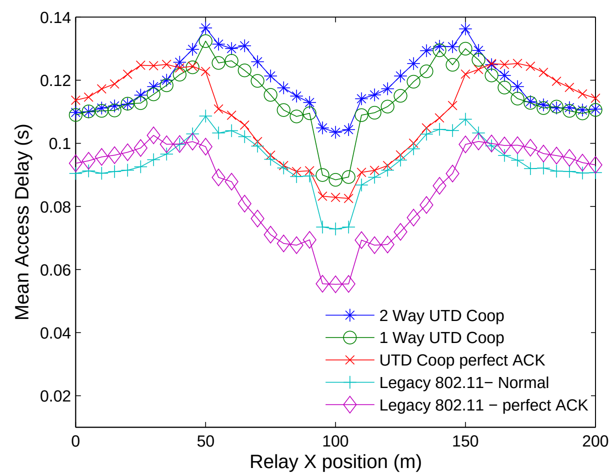

Fig. 79. Expected access delay vs. R's position along the S-D axis, S-D distance is 200 m, transmission rate is 1 Mbps, 3-way traffic

Figs. 78, 79 and 80 show throughput, expected access delay and the expected number of retransmission attempts respectively, under saturation load when the S-D distance is 200 m. R position varies along the S-D axis and also with and without the presence of perfect ACK. Perfect ACK in the sense that, ACK are never lost. S and D coordinates are $(0, 0)$ and $(200, 0)$ respectively. R coordinates are $(X, 0)$, where X is the value on the horizontal axis in both figures. Traffic is three-way, i.e., all 3 nodes S, R and D generates traffic and a fixed transmission rate of 1 Mbps for all traffic between S, R and D. In three way traffic scenario, with large distances

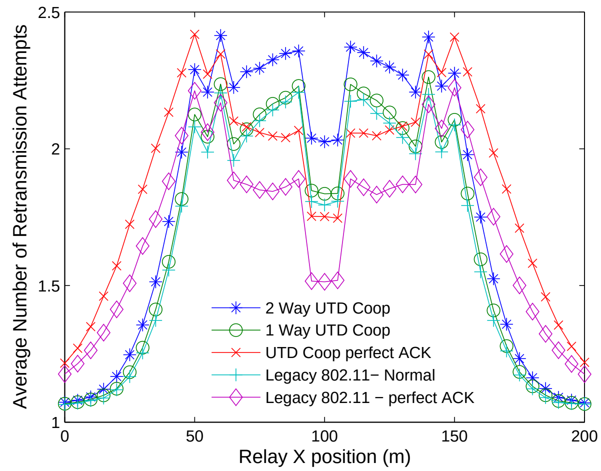

Fig. 80. Expected retransmission attempt vs. R's position along the S-D axis, S-D distance is 200 m, transmission rate is 1 Mbps, 3-way traffic

between S and D, reliable ACK even without cooperation for data frames provides a significant increase in throughput.

C. *Cooperative Protocol Results - Multiple Rates*

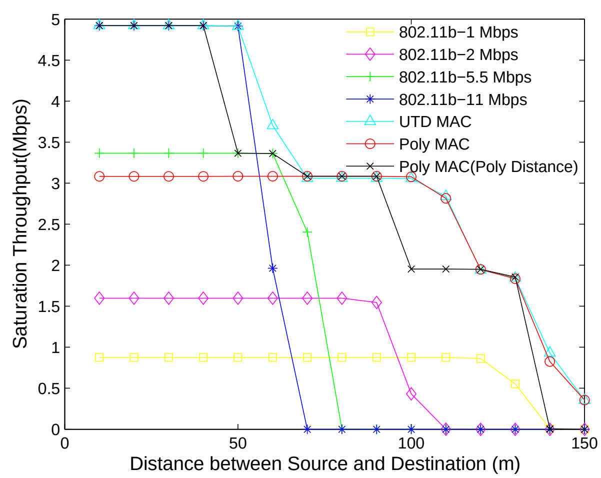

Fig. 81. Throughput vs. S-D distance, R is half way, No Fading

Fig. 81 shows the saturation throughput for the three protocols assuming that there is no fading in the channel. Four curves are reported for IEEE 802.11b for the four transmission rates 1, 2, 5.5 and 11 Mbps. It is seen that the UTD MAC performs better than IEEE 802.11b for a distance greater than 40 m. Poly MAC is advantageous for a distance of 70 m and above.

Figs. 82, 83 and 84 show saturation throughput, expected access delay and the expected retransmission attempts when the S-D distance is 100 m. R position varies along the S-D axis. S and D coordinates are $(50, 0)$ and $(150, 0)$, respectively. R coordinates are $(X, 0)$, where X is the value on the horizontal axis in both figures. Traffic is one-way. The

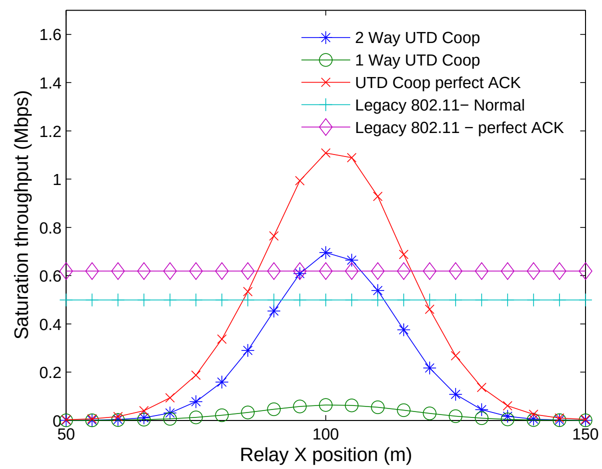

Fig. 82. Throughput vs. R's position along the S-D axis, S-D distance is 100 m, transmission rate is maximum of S-R and R-D, 1-way traffic

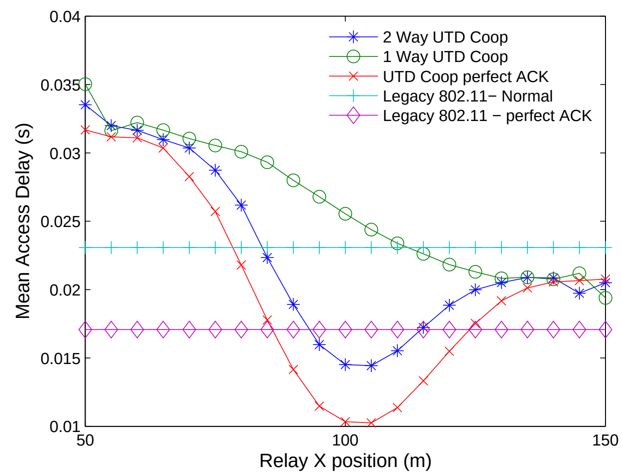

Fig. 83. Expected access delay vs. R's position along the S-D axis, S-D distance is 100 m, transmission rate is maximum of S-R and R-D, 1-way traffic

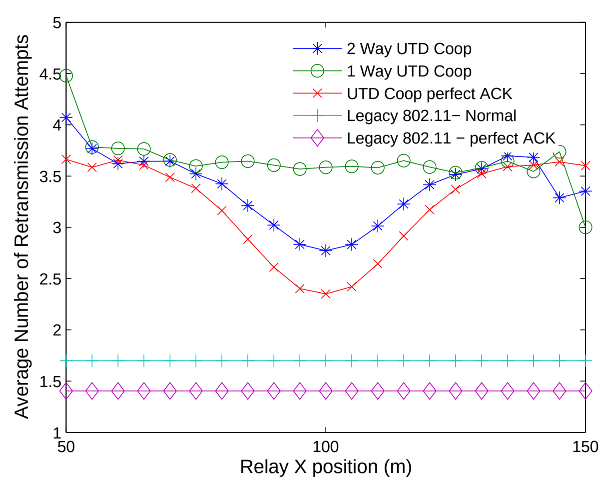

Fig. 84. Expected retransmission attempt vs. R's position along the S-D axis, S-D distance is 100 m, transmission rate is maximum of S-R and R-D, 1-way traffic

supported transmission rate for each pair S-R, R-D and S-D is determined using the distance between the nodes. The maximum of the transmission rates between S to R and R to D is used for all traffic between S, R and D. With higher transmission rate selection, throughput is suffered when the R is either close to S or D. However, maximum throughput is achieved when R is in the middle of S and D.

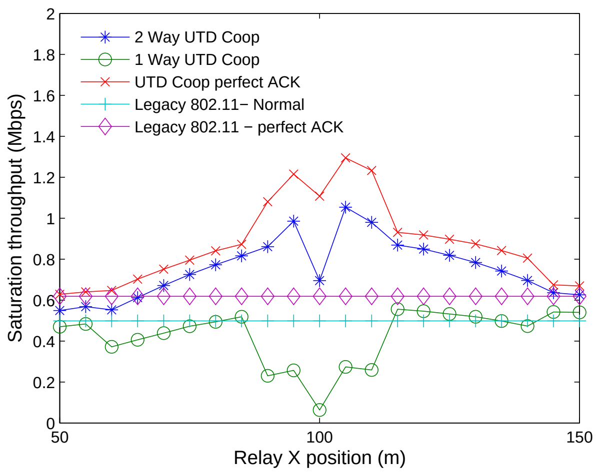

Fig. 85. Throughput vs. R's position along the S-D axis, S-D distance is 100 m, transmission rate is minimum of S-R and R-D, 1-way traffic

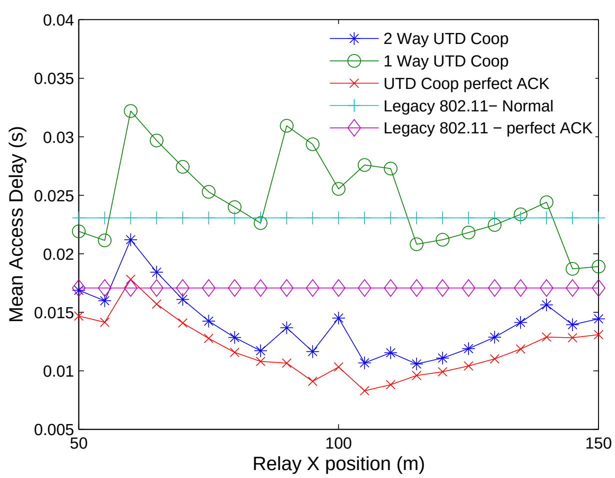

Fig. 86. Expected access delay vs. R's position along the S-D axis, S-D distance is 100 m, transmission rate is minimum of S-R and R-D, 1-way traffic

Figs. 85, 86 and 87 show throughput, expected access delay and the expected number of retransmission attempts respectively, under saturation load when the S-D distance is 100 m. R position varies along the S-D axis. S and D coordinates are $(50, 0)$ and $(150, 0)$ respectively. R coordinates are $(X, 0)$, where X is the value on the horizontal axis in both figures. Traffic is one-way. The supported transmission rate for each pair S -R, R-D and S-D is determined using the distance between the nodes. The minimum of the transmission rates between S to R and R to D is used for all traffic between

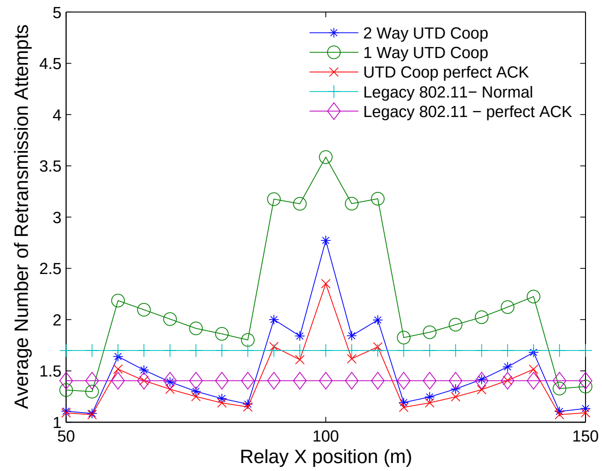

Fig. 87. Expected retransmission attempt vs. R's position along the S-D axis, S-D distance is 100 m, transmission rate is minimum of S-R and R-D, 1-way traffic

S, R and D.

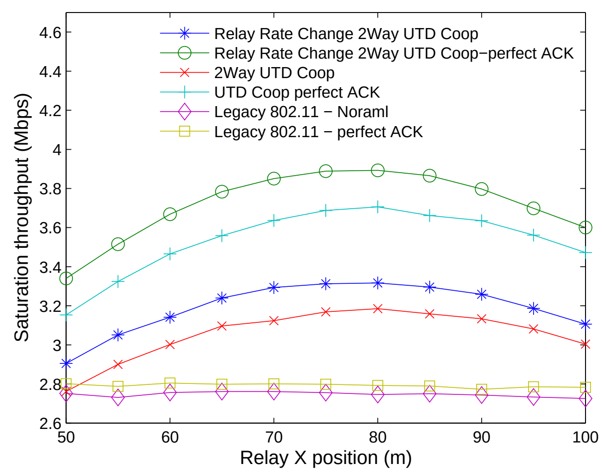

Fig. 88. Throughput vs. R's position along the S-D axis, S-D distance is 50 m, transmission rate is based on S-R and R-D, 1-way traffic

The effect of transmission rates between the nodes is studied in the following results. Figs. 88, 89 and 90 show throughput, expected access delay and the expected number of retransmission attempts respectively, under saturation load when the S-D distance is 50 m. R position varies along the S-D axis. S and D coordinates are $(50, 0)$ and $(100, 0)$ respectively. R coordinates are $(X, 0)$, where X is the value on the horizontal axis in both figures. Traffic is one-way. The supported transmission rates for each pair S -R and R-D is determined using the distance between the nodes. This is used for the traffic between S-R and R-D respectively. The traffic for S-D pair is sent at rate supported by S-R. When R is close to S, direct transmission between S-D fails most of the times. Thus most of the packets are cooperated.

Figs. 91, 92 and 93 show throughput, expected access delay and the expected number of retransmission attempts

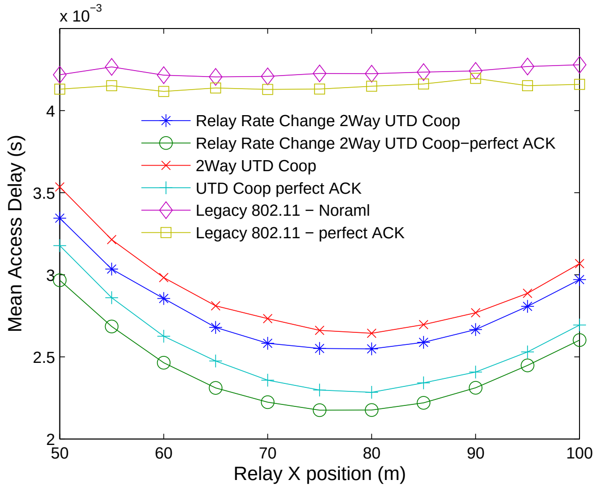

Fig. 89. Expected access delay vs. R's position along the S-D axis, S-D distance is 50 m, transmission rate is based on S-R and R-D, 1-way traffic

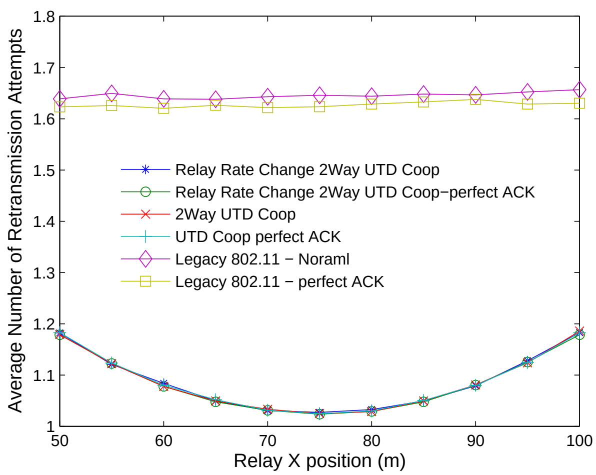

Fig. 90. Expected retransmission attempt vs. R's position along the S-D axis, S-D distance is 50 m, transmission rate is based on S-R and R-D, 1-way traffic

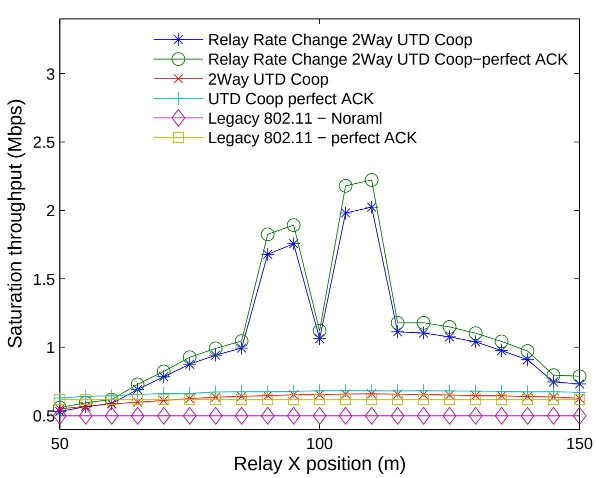

Fig. 91. Throughput vs. R's position along the S-D axis, S-D distance is 100 m, transmission rate is based on S-R and R-D, 1-way traffic

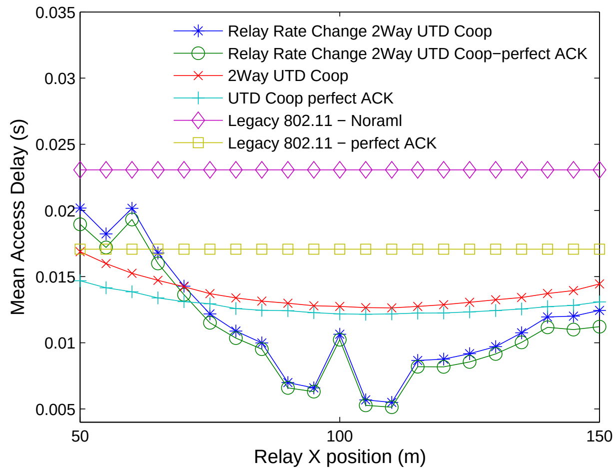

Fig. 92. Expected access delay vs. R's position along the S-D axis, S-D distance is 100 m, transmission rate is based on S-R and R-D, 1-way traffic

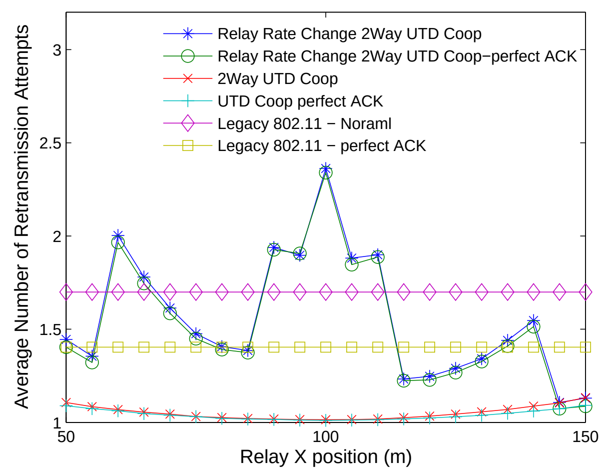

Fig. 93. Expected retransmission attempt vs. R's position along the S-D axis, S-D distance is 100 m, transmission rate is based on S-R and R-D, 1-way traffic

respectively, under saturation load when the S-D distance is 100 m. R position varies along the S-D axis. S and D coordinates are $(50, 0)$ and $(150, 0)$ respectively. R coordinates are $(X, 0)$, where X is the value on the horizontal axis in both figures. Traffic is one-way. The supported transmission rates for each pair S -R and R-D is determined using the distance between the nodes. This is used for the traffic between S-R and R-D respectively. The traffic for S-D pair is sent at rate supported by S-R. When S-D distance is very high, cooperation is at its best.

Figs. 94, 95 and 96 show throughput, expected access delay and the expected number of retransmission attempts respectively, under saturation load when the S-D distance is 150 m. R position varies along the S-D axis and also with and without the presence of perfect ACK. S and D coordinates are $(50, 0)$ and $(200, 0)$ respectively. R coordinates are $(X, 0)$, where X is the value on the horizontal axis in both figures. Traffic is one-way. The supported transmission rate for each

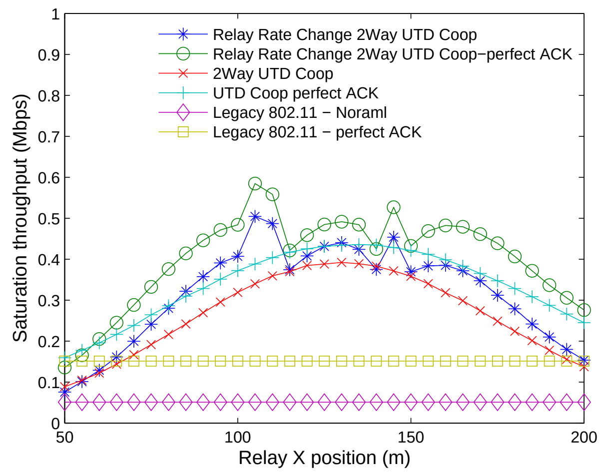

Fig. 94. Throughput vs. R's position along the S-D axis, S-D distance is 150 m, transmission rate is based on S-R and R-D, 1-way traffic

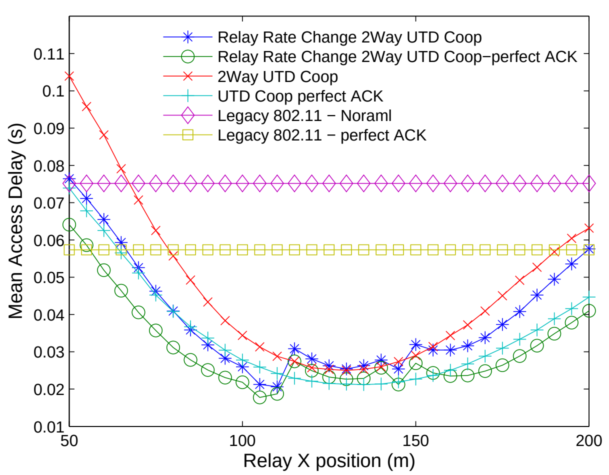

Fig. 95. Expected access delay vs. R's position along the S-D axis, S-D distance is 150 m, transmission rate is based on S-R and R-D, 1-way traffic

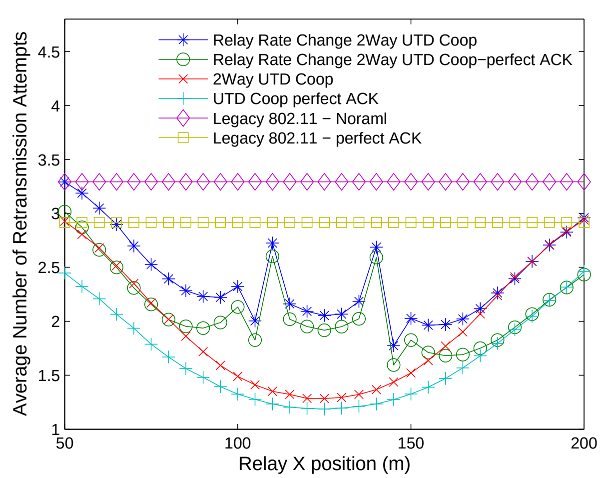

Fig. 96. Expected retransmission attempt vs. R's position along the S-D axis, S-D distance is 150 m, transmission rate is based on S-R and R-D, 1-way traffic

pair S -R and R-D is determined using the distance between the nodes. This is used for the traffic between S-R and R-D respectively. The traffic for S-D pair is sent at rate supported by S-R. Cooperation significantly helps in this case.

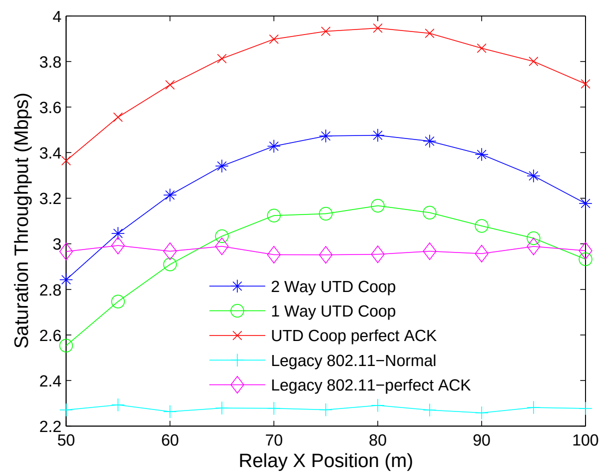

Fig. 97. Throughput vs. R's position along the S-D axis, S-D distance is 50 m, transmission rate is based on S-R and R-D, 1-way traffic

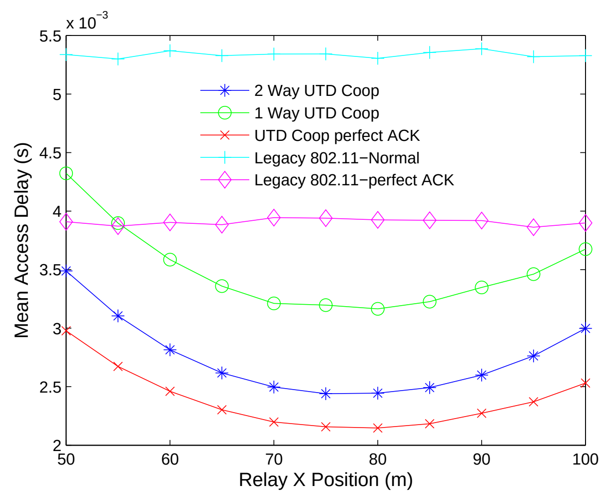

Fig. 98. Expected access delay vs. R's position along the S-D axis, S-D distance is 50 m, transmission rate is based on S-R and R-D, 1-way traffic

Figs. 97, 98 and 99 show throughput, expected access delay and the expected number of retransmission attempts respectively, under saturation load when the S-D distance is 50 m. R position varies along the S-D axis. S and D coordinates are $(50, 0)$ and $(100, 0)$ respectively. R coordinates are $(X, 0)$, where X is the value on the horizontal axis in the figures. Traffic is one-way. The supported transmission rates for each pair S -R and R-D is determined using the distance between the nodes. This is used for the traffic between S-R and R-D respectively.

Figs. 100, 101 and 102 show throughput, expected access delay and the expected number of retransmission attempts respectively, under saturation load when the S-D distance is 100 m. R position varies along the S-D axis. S and D

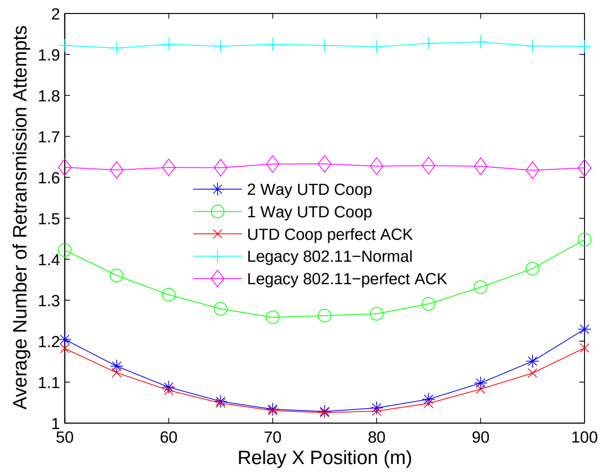

Fig. 99. Expected retransmission attempt vs. R's position along the S-D axis, S-D distance is 50 m, transmission rate is based on S-R and R-D, 1-way traffic

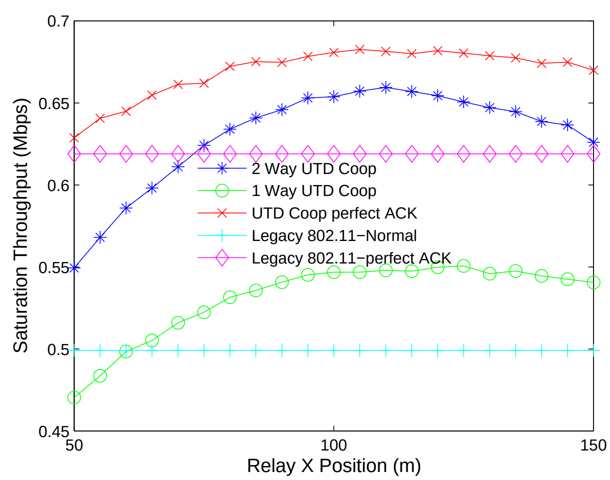

Fig. 100. Throughput vs. R's position along the S-D axis, S-D distance is 100 m, transmission rate is based on S-R and R-D, 1-way traffic

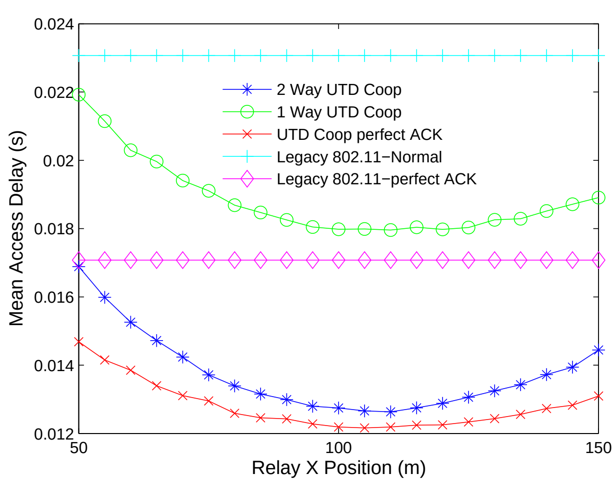

Fig. 101. Expected access delay vs. R's position along the S-D axis, S-D distance is 100 m, transmission rate is based on S-R and R-D, 1-way traffic

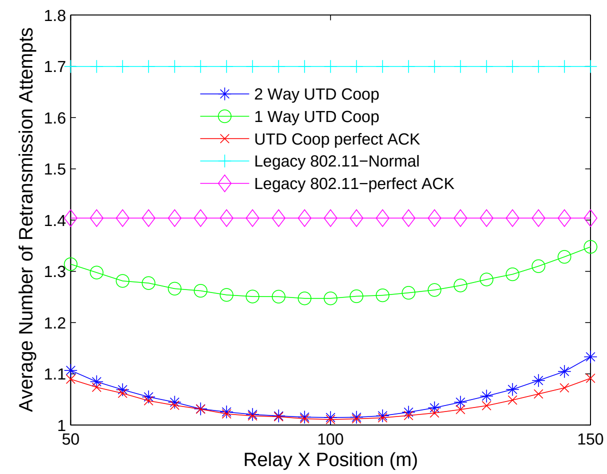

Fig. 102. Expected retransmission attempt vs. R's position along the S-D axis, S-D distance is 100 m, transmission rate is based on S-R and R-D, 1-way traffic

coordinates are $(50,0)$ and $(150,0)$ respectively. R coordinates are $(X,0)$, where X is the value on the horizontal axis in the figures. Traffic is one-way. The supported transmission rates or each pair S -R and R-D is determined using the distance between the nodes. This is used for the traffic between S-R and R-D respectively. The traffic for S-D pair is sent at rate supported by S-R. ACKs are sent at the same rate as data.

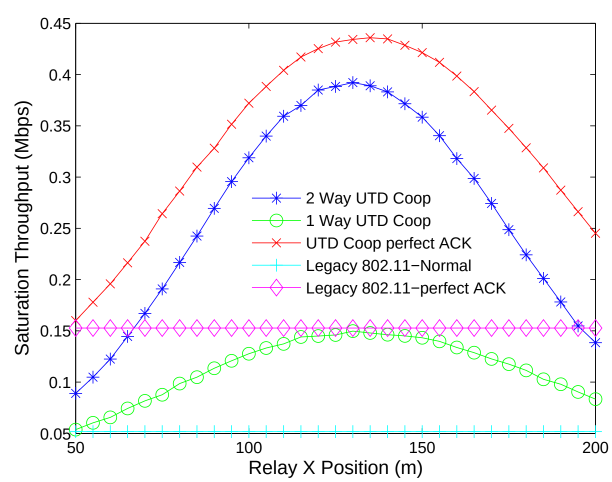

Fig. 103. Throughput vs. R's position along the S-D axis, S-D distance is 150 m, transmission rate is based on S-R and R-D, 1-way traffic

Figs. 103, 104 and 105 show throughput, expected access delay and the expected number of retransmission attempts, respectively, under saturation load when the S-D distance is 150 m. R position varies along the S-D axis. S and D coordinates are $(50,0)$ and $(200,0)$ respectively. R coordinates are $(X,0)$, where X is the value on the horizontal axis in the figures. Traffic is one-way. The supported transmission rates for each pair S -R and R-D is determined using the distance between the nodes. This is used for the traffic between S-R and R-D respectively. The traffic for S-D pair is sent at rate

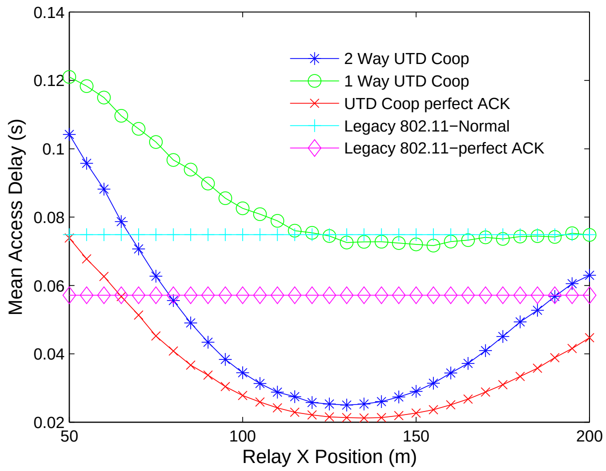

Fig. 104. Expected access delay vs. R's position along the S-D axis, S-D distance is 150 m, transmission rate is based on S-R and R-D, 1-way traffic

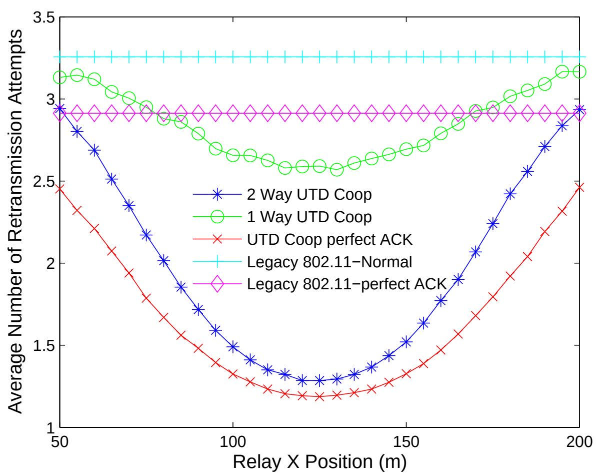

Fig. 105. Expected retransmission attempt vs. R's position along the S-D axis, S-D distance is 150 m, transmission rate is based on S-R and R-D, 1-way traffic

supported by S-R. ACKs are sent at the same rate as data.

Fig. 106 shows the throughput under saturation of the load when the S-D distance is 100 m for the Poly MAC. The channel is assumed to have no fading. R position varies along the S-D axis. S and D coordinates are $(0, 0)$ and $(100, 0)$ respectively. R coordinates are $(X, 0)$, where X is the value on the horizontal axis in both figures. Traffic is one-way.

Figs. 108 and 109 show throughput, expected access delay and the expected number of retransmission attempts respectively, under saturation load when the S-D distance is 100 m. R position varies along the S-D axis. S and D coordinates are $(0, 0)$ and $(100, 0)$ respectively. R coordinates are $(X, 0)$, where X is the value on the horizontal axis in both figures. Traffic is one-way. The throughput of the cooperative protocols is significantly affected by the Bullet Proof property between S, R and D. Significant increase in throughput is achieved with Bullet Proof ACK, i.e., we assume here that no ACK is lost.

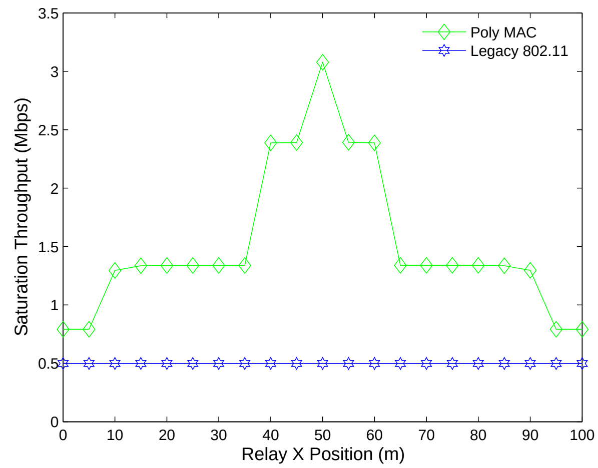

Fig. 106. Throughput vs. R's position along the S-D axis, S-D distance is 100 m,1-way traffic,Without Fading

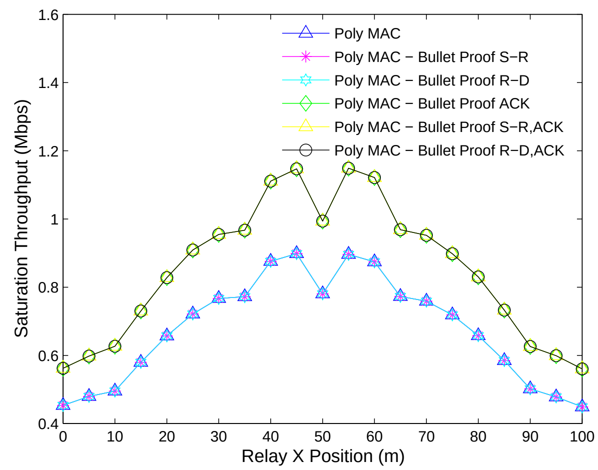

Fig. 107. Throughput vs. R's position along the S-D axis, S-D distance is 100 m, Different Combinations Of Bullet Proof Between S, R and D, 1-way traffic

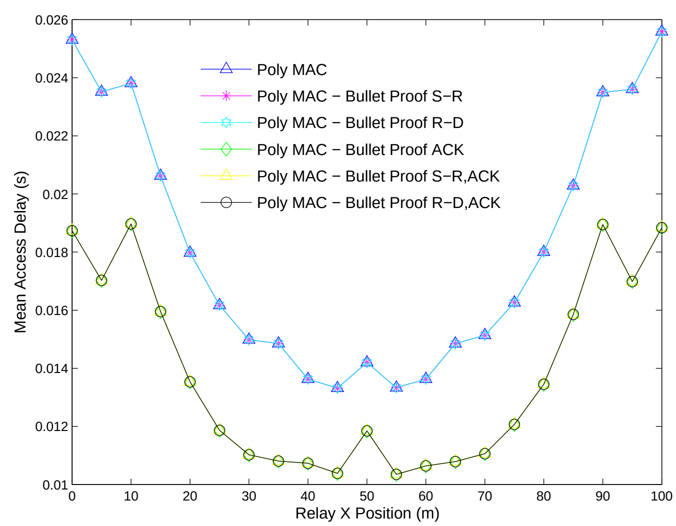

Fig. 108. Access Delay vs. R's position along the S-D axis, S-D distance is 100 m,Different Combinations Of Bullet Proof Between S, R and D,1-way traffic

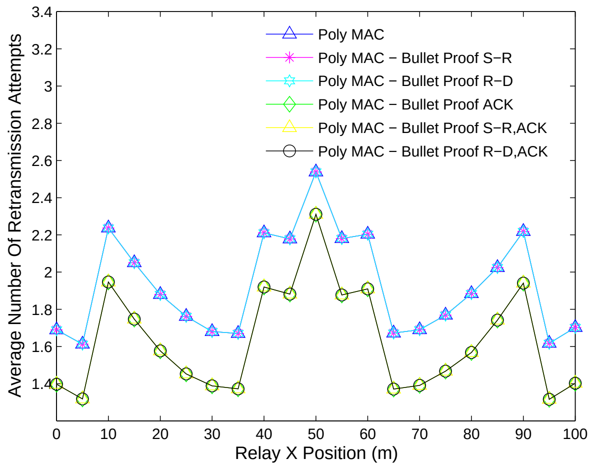

Fig. 109. Access Delay vs. R's position along the S-D axis, S-D distance is 100 m, Different Combinations Of Bullet Proof Between S, R and D,1-way traffic

IV. Conclusion

The paper investigated the use of cooperative communications techniques to enhance the IEEE 802.11b MAC protocol ability to cope with radio signal degradation in slow fading channel. Two cooperative MAC protocols were considered, i.e., the one in [8] and the one presented in the paper. Both cooperative protocols have the potential to yield higher throughput and lower latency when compared to the conventional IEEE 802.11b protocol. Alternatively, the maximum transmission span between the source and destination for a desired throughput target can be increased by up to 50% when using the cooperative protocols.

All these features may help achieve improved connectivity and network performance in ad hoc applications, where nodes' relative locations are difficult to control and predict. However, as indicated in this study, to fully harness cooperative communications in IEEE 802.11b, the cooperating nodes must be able to carefully select their transmission rates. This subject will be addressed in a future work on this topic.

References

[1] N. Kim, "IEEE 802.11 MAC performance with variable transmission rates," in *IEICE Transacation on Communications*, 2005, vol. E88-B, no. 9, pp. 3524–3531.

[2] A. Sendonaris, E. Erkip, and B. Aazhang, "User cooperation diversity part I: System description," in *IEEE Trans. Commun*, 2003, vol. 51, no. 11, pp. 1927–1938.

[3] J. N. Laneman, G. W. Wornell, and D. N. C. Tse, "An efficient protocol for realizing cooperative diversity in wireless networks," in *Proc. IEEE ISIT*, Washington, 2001, p. 294.

[4] M. Janani, A. Hedyat, T. Hunter, and A. Nosratinia, "Coded cooperation in wireless communications: Space-time transmission and iterative decoding," in *IEEE Trans. on Signal Processing*, Feb. 2004, vol. 52, no. 2, pp. 362–371.

[5] E. Zimmermann, P. Herhold, and G. Fettweis, "The impact of cooperation on diversity-exploiting protocols," in *Proc. of 59th IEEE Vehicular Technology Conference (VTC Spring)*, Feb. 2004.

[6] P. Gupta, I. Cerutti, and A. Fumagalli, "Three transmission scheduling policies for a cooperative ARQ protocol in radio networks," in *Proc. WNCG conference*, Oct. 2004.

[7] B. Zhao and M. C. Valenti, "Practical relay networks: a generalization of hybrid-ARQ," in *IEEE Journal on Selected Areas in Communications*, Jan. 2005, vol. 23, no. 1, pp. 7–18.

[8] P. Liu, Z. Tao, and S. Panwar, "A co-operative MAC protocol for wireless local area networks," in *Proc. IEEE International Conference on Communications (ICC)*, Seoul, Korea, May 2005.

[9] *Part 11: Wireless LAN Medium Access Control (MAC) and Physical Layer (PHY) Specification: High speed physical layer extenstion in the 2.4 GHz band*, Std., Sept. 1999.

[10] B. Kim, Y. Fang, and T. Wong, "Throughput enhancement through dynamic fragmentation in wireless lans," in *Proc. IEEE Transactions on Vehicular Techonology*, July 2005.